Nano Research

ISSN 1998-0124 CN 11-5974/O4
https://doi.org/10.26599/NR.2026.94909252

Research Article

Design of periodic mesoporous organosilica catalyst bearing copper phthalocyanine and quaternary ammonium for CO_2 cycloaddition

Xiufu Hua[1,2](✉), Chunfang Lai[1], Mengchi Dai[1], Yue Yu[1], Zhongyuan Liang[1], Renbo Wei[1], Lingling Wang[1](✉)

[1] Institute of Low-Carbon Technology Application, School of Chemical Engineering, Northwest University, Xi'an 710069, China

[2] Yangtze Delta Region Institute of Tsinghua University, Jiaxing 314006, China

Nano Res., **Just Accepted Manuscript** • https://doi.org/10.26599/NR.2026.94909252

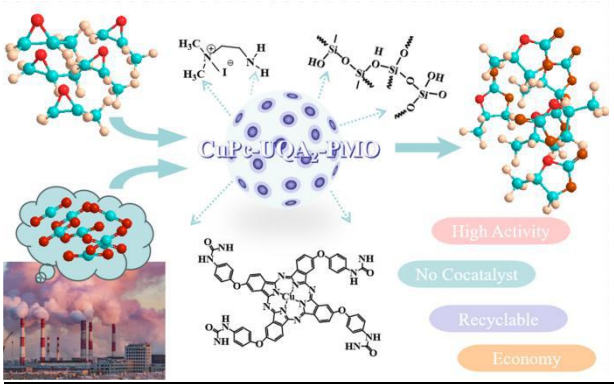
https://www.sciopen.com/journal/1998-0124 on Oct. 12, 2026

© The Authors(s)

Just Accepted

This is a "Just Accepted" manuscript, which has been examined by the peer-review process and has been accepted for publication. A "Just Accepted" manuscript is published online shortly after its acceptance,which is prior to technical editing and formatting and author proofing. Tsinghua University Press (TUP) provides "Just Accepted" as an optional and free service which allows authors to make their results available to the research community as soon as possible after acceptance. After a manuscript has been technically edited and formatted, and the page proofs have been corrected, it will be removed from the "Just Accepted" web site and published officially with volume and article number (e.g., *Nano Research*, **2025**, *18*, 94906990). Please note that technical editing may introduce minor changes to the manuscript text and/or graphics which may affect the content, and all legal disclaimers that apply to the journal pertain. In no event shall TUP be held responsible for errors or consequences arising from the use of any information contained in these "Just Accepted" manuscripts. To cite this anuscript please use its Digital Object Identifier (DOI®),which is identical for all formats of publication.

Just Accepted



A novel periodic mesoporous organosilica co-functionalized with copper phthalocyanine and quaternary ammonium salts (CuPc-UQA_2-PMO) enables highly efficient, cocatalyst-free CO_2 cycloaddition under mild conditions, driven by synergistic activation of epoxide and CO_2 at well-organized trinity active sites.

Just Accepted

Nano Research

Open Access

Research Article

Design of periodic mesoporous organosilica catalyst bearing copper phthalocyanine and quaternary ammonium for CO_2 cycloaddition

Xiufu Hua[1,2], Chunfang Lai[1], Mengchi Dai[1], Yue Yu[1], Zhongyuan Liang[1], Renbo Wei[1], and Lingling Wang[1]

[1] *Institute of Low-Carbon Technology Application, School of Chemical Engineering, Northwest University, Xi'an 710069, China*
[2] *Yangtze Delta Region Institute of Tsinghua University, Jiaxing 314006, China*

Received: 19 July 2026; **Revised:** 18 September 2026; **Accepted:** 12 October 2026

Address correspondence to Xiufu Hua, huaxf@nwu.edu.cn; Lingling Wang, wangll@nwu.edu.cn

Cite this article: *Nano Research*, 2026, 19, 94909252 https://doi.org/10.26599/NR.2026.94909252

ABSTRACT: The development of heterogeneous catalysts with high activity, stability, and co-catalyst-free operation remains a significant challenge for the sustainable conversion of CO_2 into value-added chemicals. Herein, we report a novel periodic mesoporous organosilica (PMO) heterogeneously functionalized with copper phthalocyanine (CuPc) and quaternary ammonium salts (CuPc-UQA$_2$-PMO). This catalyst integrates CuPc centers, hydrogen-bond-donating urea groups, and iodide-releasing quaternary ammonium moieties within a highly ordered mesoporous silica framework via covalent anchoring, creating a synergistic trinity active site. The resulting catalyst exhibits a well-defined spherical morphology, uniform element distribution, and a BET surface area of 714 $m^2 \cdot g^{-1}$. Under cocatalyst-free conditions (100 °C, 2.0 MPa CO_2), CuPc-UQA$_2$-PMO achieves nearly 99% yield and 100% selectivity for propylene carbonate from the cycloaddition of CO_2 and propylene oxide. Density functional theory (DFT) calculations reveal the cooperative activation of epoxide by Cu^{2+} and urea, along with the availability of I^- species from the quaternary ammonium moieties for ring-opening initiation and the synergistic adsorption/polarization of CO_2 by the π-conjugated system and quaternary ammonium cation, significantly lowers the energy barrier (24.21 $kcal \cdot mol^{-1}$ for the rate-determining step). Furthermore, the catalyst reveals excellent recyclability over five consecutive cycles without appreciable loss in activity or structural integrity, highlighting its great potential for practical applications in green carbon utilization.

KEYWORDS: metal phthalocyanine; quaternary ammonium salt; CO_2 cycloaddition; periodic mesoporous organosilica

Just Accepted

1 Introduction

With the escalating global crisis of climate change, carbon dioxide (CO_2), as the primary anthropogenic greenhouse gas, has become a focal point in sustainable development strategies. Transforming this abundant yet inert molecule into value-added chemicals not only mitigates environmental impact but also advances the vision of a closed-loop carbon economy [1-5]. Among various CO_2 utilization pathways, its catalytic cycloaddition with epoxides to form cyclic carbonates stands out due to its 100% atom economy, absence of by-products, and the broad industrial applicability of the resulting products, such as propylene carbonate (PC) which serves as a high-performance electrolyte solvent in lithium-ion batteries, a green polar aprotic solvent, and a key monomer for polycarbonates [6-10]. Despite these advantages, the practical implementation of this transformation is hindered by the inherent inertness of CO_2, which typically demands harsh conditions (high temperature and pressure) when uncatalyzed [11-13]. Therefore, developing an efficient heterogeneous catalytic system that can operate stably under mild conditions without additional co-catalysts is the key scientific issue to overcome the last mile in the industrialization of this reaction.

In recent years, various catalytic systems, such as metal-organic frameworks (MOFs), ionic liquids, covalent organic frameworks (COFs), and homogeneous metal complexes, have been explored to address the activation challenge of CO_2 and epoxides [14-20]. Some of these systems have achieved near-complete conversion of epoxides under laboratory conditions. Specifically, metal phthalocyanine compounds exhibit catalytic potential far exceeding that of conventional metal complexes in the process of CO_2 adsorption activation and directed conversion, due to their electron transport properties endowed by the large π-conjugated system within the molecule, excellent thermal/chemical stability exceeding 300 °C, and replaceable central transition metal sites as needed. Among them, copper phthalocyanine (CuPc) has been used to specifically bind to the oxygen atom of epoxides through its exposed Lewis acidic Cu^{2+} center, while utilizing the conjugated cavity of the phthalocyanine ring to complete the pre-enrichment adsorption of CO_2 [15, 21, 22]. A series of literature reports have shown that quaternary ammonium salt functional groups can stably provide free nucleophilic iodide ions (I^-), initiating a nucleophilic attack from the

backside of the less steric hindered carbon atom in the rate-determining step of the cycloaddition reaction, efficiently breaking the epoxide ring to complete ring opening. Additionally, hydrogen bond donors such as urea groups can form hydrogen bonding interactions with epoxides through N-H bond, further cooperating to weaken the bond energy of the C-O bond on the ring [23]. The combined effect of these two sites can effectively reduce the apparent activation energy of the reaction. Although these catalysts have improved reaction efficiency to some extent through the design of single active sites, they still face many common challenges: some systems require relatively harsh reaction conditions, heterogeneous catalysts have complex recycling processes, metal active sites have a high leaching risk, and some systems must additionally apply co-catalysts, homogeneous systems have high energy consumption for product and catalyst separation, etc.

The heterogenization of catalytic active centers, namely anchoring them onto porous solid supports through covalent bonding, has become a mainstream strategy in the field of CO_2 catalytic conversion [24, 25]. This strategy not only retains the high intrinsic activity of homogeneous catalysts but also endows them with process advantages such as easy separation and reusability. Mesoporous silica materials, particularly periodic mesoporous organosilicas (PMOs) are ideal supports owing to their high surface area (>800 $m^2 \cdot g^{-1}$), ordered tunable pores (2-50 nm), thermal stability (>500 °C), and abundant silanol groups. Through in-situ co-condensation or post-grafting methods, functional units such as copper phthalocyanine, quaternary ammonium salts, and hydrogen bond donors can be precisely introduced into the mesoporous framework, constructing a heterogeneous system with multi-active site synergistic catalysis [26-28]. More importantly, the spatial confinement effect of mesoporous channels can effectively regulate the spatial distance between various functional sites, promoting efficient substrate transfer between active centers, thereby significantly enhancing catalytic efficiency[29].

Building on this design principle, we herein report a series of novel metallic phthalocyanine and quaternary ammonium salt co-functionalized PMOs (MPc-UQA$_x$-PMO) synthesized via a multi-step strategy [22]. This material innovatively integrates three functional components: the Lewis acidic phthalocyanine metal active unit, the quaternary ammonium salt functional group capable of releasing nucleophilic I^-, and the hydrogen bond donor (urea group) through covalent bonding in a synergistic manner within an ordered mesoporous silica framework with a high specific surface area, achieving a 'three-in-one' multifunctional integration [30, 31]. This design not only successfully addresses the challenge of difficult recovery of homogeneous catalysts but also constructs a synergistic catalytic network with multiple active sites within the same nanoscale space, enabling efficient driving of the cycloaddition reaction between CO_2 and epoxides [32, 33]. Through systematic tuning of the metal type and active site ratio, this study clarified the optimal catalytic structure-activity relationship, providing a novel design approach for high-stability recyclable catalysts tailored for CO_2 utilization and further expanding the application boundaries of multifunctional ordered mesoporous materials in green chemistry and CO_2 utilization.

2 Experimental

2.1 Materials

4-Aminophenyl isocyanate, 4-nitrophthalonitrile, and N,N-diisopropylethylamine (DIPEA) were purchased from Adamas Reagents. Isocyanatopropyltriethoxysilane, hexadecyltri-methylammonium bromide (CTAB), bis(tri-ethoxysilyl)ethane (BTEE), and 3-chloropropyl-triethoxysilane (CPTES) were obtained from Macklin reagents. Propylene oxide (PO) and other solvents were purchased locally. More detailed information on reagents can be found in the Supporting Information. All reagents were used as received without further purification.

2.2 Synthesis of tetra(4-aminophenoxy)-phthalocyanine metal complexes (MTAPPc, M = Cu, Co, Zn)

A representative synthesis of CuTAPPc was carried out as follows: 4-Aminophthalonitrile (4-APN, 10.0 g) and copper(II) chloride ($CuCl_2$, 1.0 g) were dissolved in N,N-dimethylacetamide (DMAc, 40 mL) under mechanical stirring. The mixture was heated to 165 °C and refluxed for 4 h under nitrogen atmosphere. After cooling to room temperature, the green precipitate was collected by filtration and washed thoroughly with deionized water to remove unreacted $CuCl_2$. The crude product was then recrystallized from methanol by heating under reflux for 10 min, followed by hot filtration. This purification process was repeated twice. The final green powder was dried under vacuum at 80 °C overnight to afford CuTAPPc. Analogous procedures were employed to synthesize CoTAPPc and ZnTAPPc using cobalt(II) chloride or zinc(II) chloride as the metal source, respectively.

2.3 Synthesis of phthalocyanine-based organo-silane precursors (MPcUTES)

In a typical procedure for CuPcUTES, CuTAPPc (2.0 g), DIPEA (112.0 mg), and isocyanatopropyl-triethoxysilane (3.6 g) were added into anhydrous tetrahydrofuran (THF, 15 mL). The reaction mixture was stirred under nitrogen atmosphere at 80 °C for 12 h. After completion, the solvent was removed by rotary evaporation. The residue was washed sequentially with ethyl acetate and ethanol (3 × 100 mL), and the resulting solid was dried under vacuum at 80 °C for 24 h to yield the green product CuPcUTES. Similarly, CoPcUTES and ZnPcUTES were synthesized using CoTAPPc or ZnTAPPc as starting materials.

2.4 Preparation of chloro-functionalized PMO (MPc-UCl$_x$-PMO)

The preparation of CuPc-UCl$_2$-PMO was typically conducted via a co-condensation method. CTAB (1.4 g) was dissolved in deionized water (665 mL) containing NaOH (2 M, 5 mL), and the solution was heated to 80 °C with vigorous stirring (850 rpm) for 50 min. Subsequently, a mixture of CuPcUTES (47.2 mg), BTEE (142.0 mg), and CPTES (47.2 mg) pre-dissolved in dimethyl sulfoxide (DMSO, 3 mL) was slowly added into the

Just Accepted

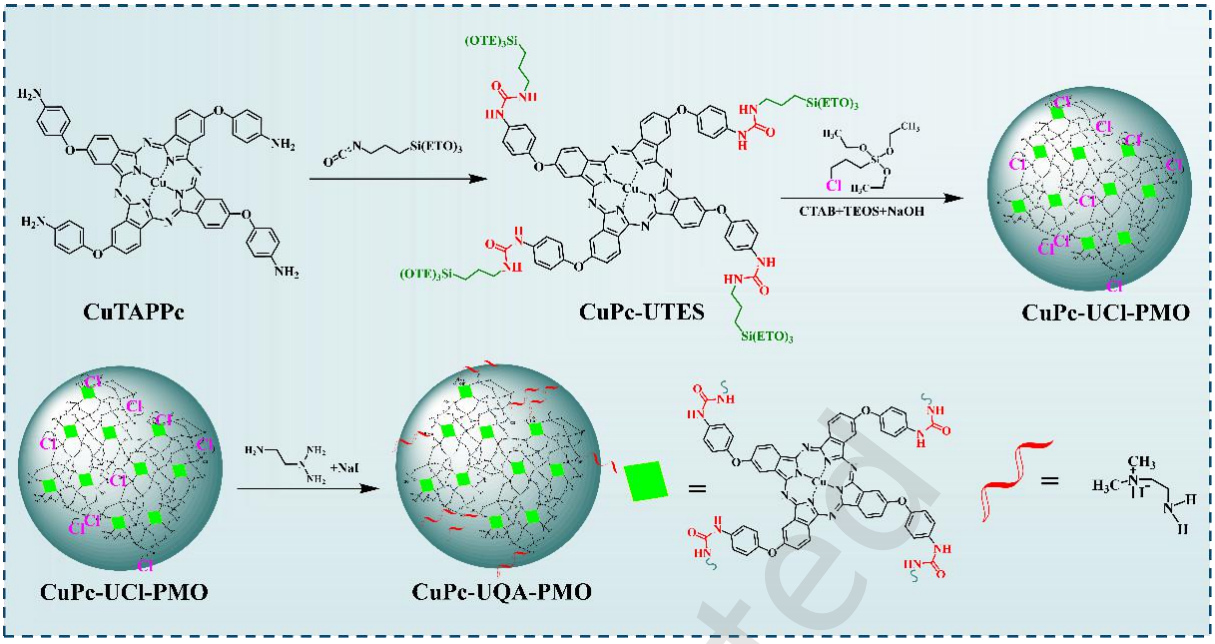


Figure 1. Schematic diagram for the MPc-UQA$_x$-PMO.

above solution. The reaction continued at 80 °C for another 2 h. The resulting solid was collected by centrifugation. To remove the CTAB template, the as-synthesized material was extracted with a 6.0 g/L ammonium nitrate/ethanol solution at 50 °C under ultrasonication for 30 min, followed by centrifugation (11,000 rpm, 20 min). This washing process was repeated until no residual surfactant was detected. The purified product was washed with ethanol, filtered, and dried under vacuum to obtain the green solid denoted as CuPc-UCl$_2$-PMO.The subscript 2 denotes the molar equivalents of CPTES relative to CuPcUTES used in the co-condensation step, which directly controls the density of chloro-functional groups and, subsequently, quaternary ammonium functionalities in the final PMO framework. By varying the amount of CPTES (0, 23.6, 47.2 or 70.8 mg), a series of samples with different chloro-functional group contents (CuPc-UCl$_x$-PMO) (x=0,1,2,3) were prepared. Controlling samples including UCl-PMO (without phthalocyanine) and pure PMO (without any functional groups) were also synthesized following the same protocol.

2.5 Synthesis of MPc and quaternary ammonium functionalized catalysts (MPc-UQA$_x$-PMO)

The synthesis of CuPc-UQA$_2$-PMO was carried out by reacting CuPc-UCl$_2$-PMO (0.1 g), NaI (0.1 mmol), and N,N-dimethylethylenediamine (0.1 mmol) in anhydrous DMAc (40 mL) under N$_2$ at 110 °C for 24 h. After cooling, the solid product was isolated by centrifugation and washed repeatedly with ethanol (3 times), deionized water (3 times), and finally ethanol again (3 times). The final product was dried under vacuum at 80 °C and designated as CuPc-UQA$_2$-PMO. Analogously, CuPc-UQA$_1$-PMO, CuPc-UQA$_3$-PMO, CoPc-UQA$_2$-PMO, and ZnPc-UQA$_2$-PMO were synthesized using corresponding precursor materials. The subscript x in UQA$_x$ carries the same meaning as in UCl$_x$, namely the molar equivalents of CPTES relative to CuPcUTES.

2.6 Catalytic evaluation for CO_2 cycloaddition

The catalytic activity of the as-synthesized catalysts toward the cycloaddition of CO_2 and epoxides was evaluated in a batch-type stainless steel autoclave. Prior to each reaction, the reactor was flushed three times with CO_2 to eliminate residual air. Subsequently, a predetermined amount of catalyst and propylene oxide (PO, 5 mmol) were loaded into the reactor. The system was then pressurized with CO_2 to the desired initial pressure and heated to the target temperature under magnetic stirring. After the specified reaction time, the reactor was rapidly cooled to room temperature using an ice-water bath, and the internal pressure was slowly released. The reaction mixture was carefully transferred out of the reactor with ethyl acetate or toluene and centrifuged to separate the solid catalyst. The recovered catalyst was washed thoroughly with anhydrous ethanol via ultrasonication, then dried under vacuum at 80 °C for 12 h before being weighed and used in the subsequent recycling run. This drying protocol was strictly followed for all five recycling tests to eliminate any residual solvent or moisture and to minimize moisture-induced deactivation. The dried catalyst was then used directly in the next cycle without any further treatment.

2.7 Characterization

Multiple methods such as Fourier transform infrared spectroscopy (FT-IR), X-ray photoelectron spectroscopy (XPS), scanning electron microscopy (SEM) and energy dispersive spectroscopy (EDS), nitrogen adsorption-desorption isotherms (BET), thermogravimetric analysis (TGA), and ultraviolet-visible absorption spectroscopy (UV-vis) were used to systematically characterize the structure, morphology, elemental composition, and thermal stability of the prepared catalysts and their precursors. The specific test parameters are detailed in the Supporting Information.

3 Results and discussion

3.1 Preparation of the MPc-UQA$_x$-PMO catalysts

Just Accepted

A series of novel multifunctional PMO-based heterogeneous catalysts, designated as MPc-UQA$_x$-PMO (M = Cu, Co, Zn; x = 0, 1, 2, 3), were rationally designed and successfully constructed through a multi-step, controllable synthetic strategy in this study. These catalysts integrate three functional components, Lewis acidic CuPc, H-bond donating urea, and I^--releasing quaternary ammonium, within a ordered mesoporous framework, achieving a trinity catalytic architecture tailored for the cycloaddition of CO_2. The synthesis proceeds through four sequential steps, as illustrated in Figure 1 using MPc-UQA$_x$-PMO as an example. First, CuTAPPc were synthesized via cyclotetramerization of 4-APN with corresponding Cu salts. Second, the CuTAPPc units were functionalized with triethoxysilyl groups, yielding the silylated intermediate CuPcUTES. Then, the CuPcUTES was incorporated into the mesoporous silica skeleton via co-condensation with bis(triethoxysilyl)ethane (BTEE) and varying amounts of 3-chloropropyltriethoxysilane (CPTES) in the presence of CTAB. This sol-gel process, conducted under basic conditions at 80 °C, yielded chloro-functionalized hybrid materials denoted as CuPc-UCl$_x$-PMO. Finally, the chloride-terminated materials were subjected to a nucleophilic substitution reaction with sodium iodide (NaI) and N,N-dimethylethylenediamine, converting the -CH_2Cl groups into iodide-containing quaternary ammonium moieties, offering the target catalysts CuPc-UQA$_x$-PMO. Notably, this modular synthetic route not only enables precise structural engineering of active sites but also ensures their strong covalent attachment to the inorganic framework, thereby enhancing the catalysts' stability and recyclability. More importantly, it establishes a versatile platform for constructing multifunctional heterogeneous catalysts with spatially organized, synergistic active centers, ideal for promoting complex cascade reactions such as the CO_2-epoxide cycloaddition.

3.2 Characterization of the MPc-UQA$_x$-PMO catalysts

To systematically verify the successful synthesis and structural integrity of the target MPc-UQA$_x$-PMO catalysts and their key intermediates, a comprehensive suite of analytical techniques was employed to investigate their chemical composition, morphological features, and porous architecture. The characterization focused primarily on CuPc-UQA$_2$-PMO, while other members of the series were indicated through consistent synthetic pathways and representative analyses.

The synthesis commenced with the preparation of CuTAPPc, which is indicated by ^{1}H NMR and FTIR spectra, where characteristic signals corresponding to aromatic protons and amino groups are observed, with peak positions fully consistent with the theoretical framework (Figures S1,S2). Subsequently, CuTAPPc was functionalized with (3-triethoxysilylpropyl) isocyanate, yielding the intermediate CuPcUTES. The success of this coupling reaction is evidenced by FTIR spectroscopy: new absorption bands appear at 2800-3000 cm^{-1}, resulting from symmetric and asymmetric stretching of -CH_2- groups, along with distinct Si-O-Si vibrations at 1035 and 1165 cm^{-1} (Figure S3) [27]. Moreover, UV-vis spectrum of CuPcUTES exhibits two characteristic

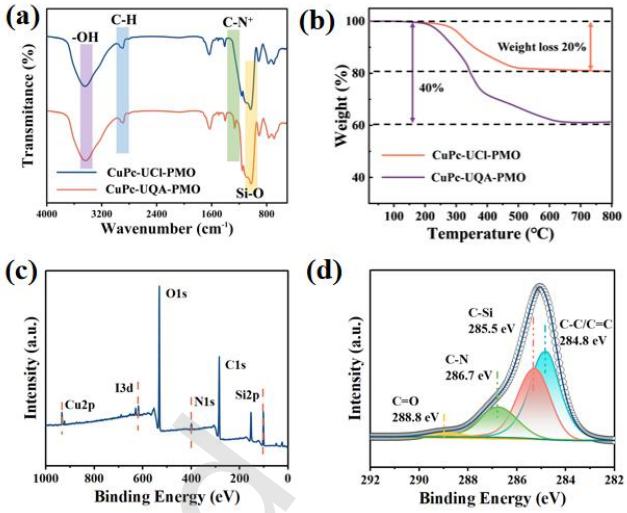


Figure 2. FTIR spectra (a) and TGA curves (b) of CuPc-UCl$_2$-PMO and CuPc-UQA$_2$-PMO; XPS spectrum (c) and C1s spectrum (d) of CuPc-UQA$_2$-PMO.

absorption bands at 618 and 680 nm (Figure S4), corresponding to the Q-band of phthalocyanine copper, indicating that the core conjugated structure remained intact during functionalization [34]. The FTIR spectrum of CuPc-UCl$_2$-PMO (Figure 2a) displays strong absorptions at 3430, 1035, and 1165 cm^{-1}, suggesting the formation of the silica-based matrix. Additionally, characteristic peaks associated with -CH_2-, C=O, N-H, and aromatic rings are retained, indicating the successful incorporation of organic functionalities [35]. The preservation of the phthalocyanine unit is further verified by UV-vis spectrum, which shows clear Q-band absorptions at the expected wavelengths (Figure S5a). TGA curve of CuPc-UCl$_2$-PMO reveals a high residual mass of ~80 wt% at 800 °C (Figure 2b), indicative of a robust inorganic silica framework. Analogous results are obtained for CoPc-UCl$_2$-PMO and ZnPc-UCl$_2$-PMO (Figures S6,S7), whose UV-vis and TGA profiles closely resemble those of CuPc-UCl$_2$-PMO, supporting the general applicability of the synthetic strategy across different metal centers. In contrast, control samples such as PMO and UCl-PMO exhibit higher thermal stability (residual masses approaching 90-100 wt% (Figures S8,S9), further validating the contribution of organic moieties to the observed weight loss behavior.

The final transformation involved the conversion of terminal chloro groups into iodide-containing quaternary ammonium salts via nucleophilic substitution, affording the target catalyst CuPc-UQA$_2$-PMO. The successful introduction of quaternary ammonium functionality is clearly revealed by FTIR spectrum, where a new strong band emergs at 1267 cm^{-1} (Figure 2a), attributing to C-N$^+$ stretching vibration. Concurrently, TGA analysis shows a slightly reduced residue compared to CuPc-UCl$_2$-PMO (Figure 2b), resulting from the worse thermal stability of organic ammonium component, which is a further evidence of its presence within the framework [36]. The full-scan XPS spectrum (Figure 2c) unambiguously detects signals from O, C, N, Si, Cu, and I, suggesting the hybrid organic-inorganic nature of CuPc-UQA$_2$-PMO. Peaks for O1s and Si2p indicate the continuity of the siliceous network, while Cu2p signals verifies the

Just Accepted

retention of the phthalocyanine-bound Cu^{2+} active center. Deconvolution of the C1s spectrum (Figure 2d) resolves four components: 284.8 eV (C=C/C–C, aromatic carbon), 285.5 eV (C–Si), 286.7 eV (C–N, from both phthalocyanine and amine linkages), and 288.8 eV (C=O) [37], collectively supporting the integration of multiple functional units. The N1s spectrum (Figure S10a) is fitted to three peaks: 399.8 eV (C–N), 400.5 eV (N–H), and 402.1 eV ($C-N^+$), being definitive evidence of successful quaternization. Furthermore, I3d spectrum (Figure S10b) displays characteristic doublets at 619 eV (I3d5/2) and 631 eV (I3d3/2), suggesting the incorporation of I- counterions[22]. Notably, UV-vis spectroscopy still exhibits typical Q-bands (Figure S11), demonstrating that the phthalocyanine core remains structurally stable throughout the multi-step synthesis.

As shown in Figure 3a-3c, CuPc-UQA$_2$-PMO exhibits uniform spherical morphology with smooth surfaces and well-defined particle boundaries, suggesting excellent morphological control during synthesis. High-magnification images reveal no significant cracks or aggregation, likely due to the cross-linked silica network and improved dispersibility imparted by the quaternary ammonium modification. EDS elemental mapping (Figure 3d-3h) visually indicates the homogeneous spatial distribution of C, N, O, Cu, and I throughout the spherical particles. Carbon and nitrogen signals originate from the organic ligands, phthalocyanine ring, and quaternary ammonium groups; oxygen reflects the continuous SiO_2 backbone; copper mapping indicates uniform anchoring of the phthalocyanine units within the mesoporous framework; and the co-localization of iodine supports the uniformity of quaternary ammonium functionalization. Additionally, the copper content in CuPc-UQA$_2$-PMO was determined using an atomic absorption spectroscopy after acid digestion. The sample was dissolved in a mixture of HNO_3 and HF, followed by dilution with deionized water. The Cu loading was found to be 0.42 mmol·g^{-1}. These results support the formation of a chemically homogeneous material at the microscale.

Nitrogen adsorption-desorption isotherms (Figure 3i) display a typical Type IV profile with an H1-type hysteresis loop, characteristic of materials with well-ordered mesoporous structures. The BET specific surface area reaches up to 714 $m^2 \cdot g^{-1}$, providing abundant accessible sites for catalytic reactions. The pore size distribution (Figure 3j) shows a narrow distribution centered in the micropore-to-mesopore range, further indicating the development of a highly porous architecture. Such a combination of high surface area and ordered porosity facilitates efficient mass transport and substrate diffusion, creating favorable conditions for heterogeneous catalysis. In summary, a battery of complementary characterization techniques has conclusively supported the successful construction of the CuPc-UQA$_2$-PMO catalyst, from molecular-level functional group incorporation to nanoscale elemental homogeneity and macroscopic mesoporous architecture. For the other series of catalysts, such as CuPc-UQA$_1$-PMO, CuPc-UQA$_3$-PMO, CoPc-UQA$_2$-PMO, and ZnPc-UQA$_2$-PMO, although only preliminary tests such as UV-vis and TGA were conducted (Figures S12-S18), their spectral characteristics are highly similar to those of CuPc-UQA$_2$-PMO. Combined with the unified synthesis strategy, it can be reasonably assumed that their structures have also been successfully constructed. These results indicate the effective immobilization of phthalocyanine copper Lewis acid sites, hydrogen-bond-donating urea groups, and iodide-releasing quaternary ammonium functionalities within a robust, high-surface-area periodic mesoporous silica framework. This structural foundation underpins its exceptional performance in the subsequent CO_2 cycloaddition reactions.

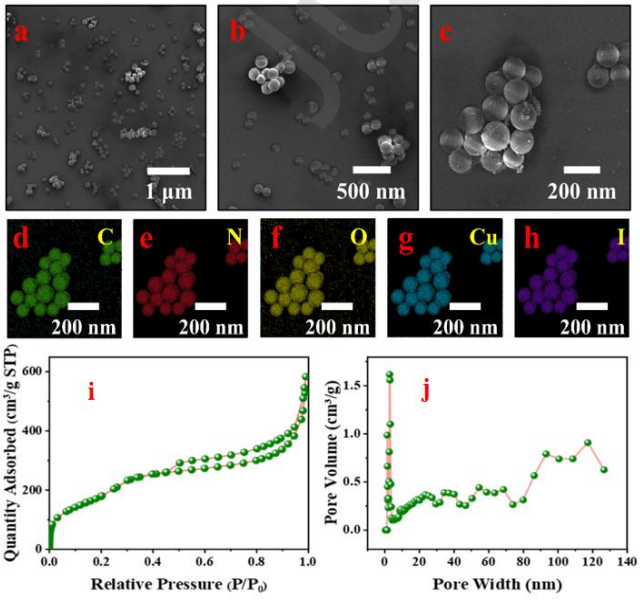


Figure 3. SEM images of CuPc-UCl$_2$-PMO (a-c); SEM mapping images of CuPc-UCl$_2$-PMO (d-h); N_2 adsorption-desorption isotherms (e) and pore size distribution (f) of CuPc-UCl$_2$-PMO.

Table 1 Comparative catalytic performance for CO_2 and PO cycloaddition over different catalysts.

Entry	Catalyst	Co-catalyst	Yield (%)[b]	Selectivity (%)[b]
1	-	-	0	-
2	CuTAPPc	-	36	99
3	CuPc-UCl$_2$-PMO	-	15	99
4	CuPc-UCl$_0$-PMO	-	17	99
5	CuPc-UQA$_0$-PMO	-	17	99
6	TBAI	-	28	99
7	CuPc-UCl$_2$-PMO	TBAI[c]	83	99
8	UCl-PMO	-	8	99
9	PMO	-	0	-
10	CuPc-UQA$_2$-PMO	-	92	99
11	CuPc-UQA$_2$-PMO	TBAI[c]	99	99
12	CuPc-UQA$_1$-PMO	-	90	99
13	CuPc-UQA$_3$-PMO	-	91	99
14	CoPc-UQA$_2$-PMO[d]	-	88	99
15	ZnPc-UQA$_2$-PMO[e]	-	90	99

[a]: Reaction conditions: 1.5 MP, 90 ℃ for 8 h and catalyst: 7.0 wt% of PO.
[b]: Determined by GC analysis.
[c]: Cocatalyst: 1.0 mol% of PO.
[d]:CoPc-UQA-PMO, 6.4 wt% of PO.
[e]:CoPc-UQA-PMO, 7.1 wt% of PO.

3.3 Catalytic performance evaluation of the MPc-UQA$_x$-PMO catalysts

The CO_2/PO cycloaddition performance of the MPc-UQA$_x$-PMO catalysts was systematically evaluated under mild conditions (90 °C, 1.5 MPa, 8 h). As summarized in Table 1, controlling experiments were executed to elucidate the

Just Accepted

contribution of each functional component and support design rationale. In the absence of any catalyst (entry 1), no detectable amount of PC was formed, suggesting the necessity of a catalytic system for this transformation [38-40]. When the homogeneous counterpart, CuTAPPc, was employed (entry 2), a moderate yield of 36% is achieved with nearly complete selectivity (>99%), demonstrating the intrinsic catalytic activity of the phthalocyanine core. In contrast, PMO and UCl-PMO exhibit negligible activity (entries 7 and 8), indicating that the silica framework alone or the presence of chloroalkyl groups cannot effectively promote the reaction. Notably, when the phthalocyanine unit was immobilized within the mesoporous silica matrix, forming CuPc-UCl_2-PMO and CuPc-UCl_0-PMO, the catalysts show modest activity with PC yields of 15% and 17%, respectively (entries 3 and 4). This result indicates the feasibility of heterogenizing molecular active sites while retaining partial catalytic function. More importantly, the addition of TBAI as an external cocatalyst to the CuPc-UCl_2-PMO system significantly enhanced the yield to 83% (entry 6), far exceeding the performance of TBAI alone (28%, entry 5) [41]. This synergistic effect suggests that the immobilized Cu^{2+} center likely activates the epoxide via Lewis acid coordination, while the exogenous I- serves as a nucleophile to initiate ring-opening. These findings strongly support our design strategy: the low activity of CuPc-UQA_0-PMO (17%, entry 4), which lacks the I^- source, underscores the critical role of in situ I^- release in initiating ring-opening. Meanwhile, the dramatic activity enhancement of CuPc-UCl_2-PMO from 15% to 83% upon addition of TBAI (entries 3 and 6) demonstrates the synergistic interplay between the Cu^{2+} Lewis acid site and exogenous I^- . Together, these experimental results validate the necessity of integrating both functionalities into one framework for co-catalyst-free operation.To test this hypothesis, the quaternary ammonium-functionalized catalyst CuPc-UQA_2-PMO was evaluated without any additional additives. Remarkably, it delivers a high PC yield of 92% with >99% selectivity (entry 9), surpassing its precursor CuPc-UCl_2-PMO and indicating that the tethered quaternary ammonium group can intrinsically release I- to serve as an internal nucleophilic promoter. Further improvement to 99% yield is realized upon adding TBAI (entry 10), underscoring the compatibility and cooperativity between the built-in and external iodide sources.

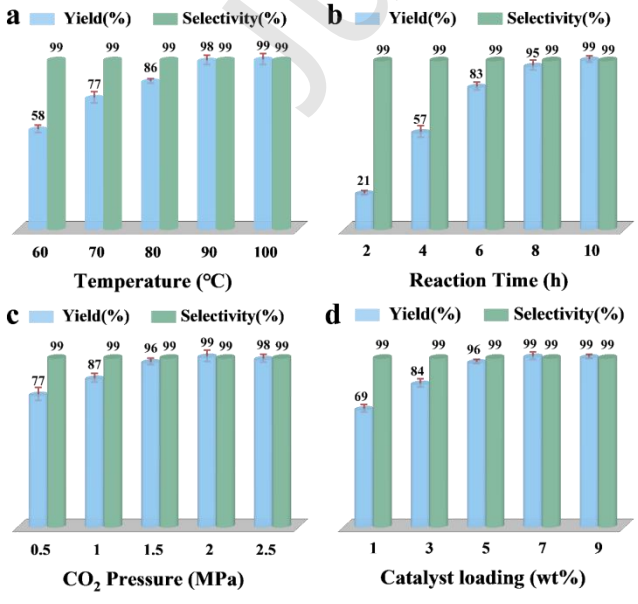


Figure 4. Influence of reaction parameters, (a) reaction temperature, (b) reaction time, (c) CO_2 pressure, (d) catalyst loading on the PC yield and selectivity.

To identify the optimal balance between the density of nucleophilic sites and structural accessibility, a series of catalysts with varying degrees of quaternary ammonium functionalization, denoted as CuPc-UQA_x-PMO (x = 1, 2, 3), were synthesized and evaluated. As shown in Table 1, the catalytic performance exhibits a maximum at x = 2, delivering the highest propylene carbonate yield (92%). While both CuPc-UQA_1-PMO and CuPc-UQA_3-PMO also show high activity, their slightly lower yields suggest that insufficient iodide release (x=1) or potential site crowding (x=3) may limit efficiency. Hence, the x = 2 formulation was selected as the optimal structure for further characterization and reaction optimization. Additionally, the influence of the central metal ion in the phthalocyanine unit was examined by preparing analogous CoPc-UQA_2-PMO and ZnPc-UQA_2-PMO (entries 13 and 14). Both display excellent catalytic activity (88% and 90%, respectively), yet remain below the performance of the Cu-based analogue. The results collectively indicate Cu^{2+} center plays a superior role in activating epoxide substrate, likely due to its optimal Lewis acidity and electronic interaction with the ligand environment, making CuPc-UQA_2-PMO the most promising candidate for subsequent studies.

With CuPc-UQA_2-PMO identified as the optimal catalyst, parametric optimization was conducted to evaluate the effects of temperature, time, CO_2 pressure, and catalyst loading. The yield increases sharply from 58% at 60 °C to 98% at 90 oC, and plateaus at 99% when the temperature reached 100 °C (Figure 4a), consistent with Arrhenius-type behavior where elevated temperature accelerates the reaction rate until thermodynamic equilibrium is approached. Prolonging the reaction time from 2 to 10 hours led to a steady increase in yield from 21% to 99% (Figure 4b), indicating a typical progression from kinetic control toward full conversion. Similarly, increasing the CO_2 pressure from 0.5 to 2.0 MPa boosted the yield from 77% to 99% (Figure 4c), attributing to improved CO_2 solubility and mass transfer within the mesopores; further pressurization to 2.5 MPa provided no additional benefit, suggesting saturation of CO_2 dissolution at 2.0 MPa. The catalyst loading also had a pronounced effect: raising the amount from 1 wt% to 7 wt% relative to PO increased the yield from 69% to 99% (Figure 4d), beyond which no significant enhancement was observed, implying sufficient availability of active sites under these conditions. Under the optimized reaction parameters, 100 °C, 2.0 MPa CO_2, 7.0 wt% catalyst loading, and 10 h reaction time, the CuPc-UQA_2-PMO catalyst achieves quantitative yield (99%) and near-perfect selectivity (99%) in the synthesis of PC. This performance not only highlights the high atom economy and energy efficiency of the process but also establishes a robust foundation for potential scale-up applications. Based on the

Just Accepted

measured Cu content of 0.42 mmol·g^{-1} the catalyst achieves a TON of ~1178 and a TOF of ~118 h^{-1}, demonstrating high catalytic efficiency per Cu active site. A comparison with representative heterogeneous catalysts reported for CO_2/epoxide cycloaddition is provided in Table S1. CuPc-UQA$_2$-PMO affords 99% PC yield and 99% selectivity under solvent-free and cocatalyst-free conditions, showing competitive performance among multifunctional heterogeneous systems. In particular, representative functionalized PMO catalysts can achieve similarly high carbonate yields but commonly employ an external halide cocatalyst, whereas CuPc-UQA$_2$-PMO contains the iodide functionality within the catalyst. Overall, the comparison highlights the combination of competitive catalytic performance, cocatalyst-free operation, and an ordered mesoporous organosilica architecture with multiple integrated functional sites in the present system.

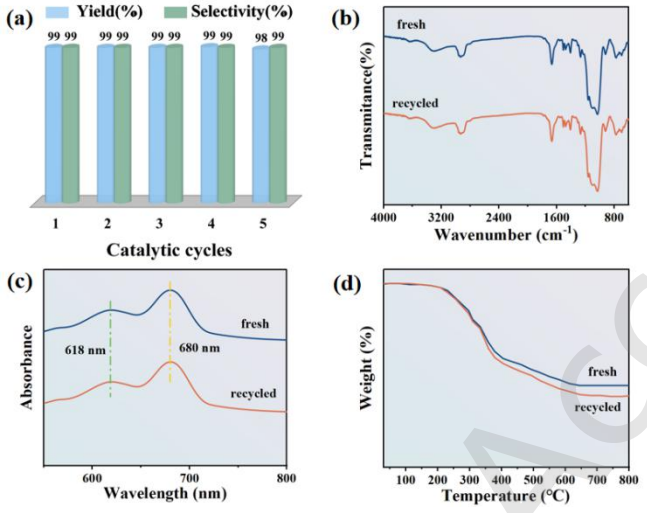


Figure 5. (a) Catalytic cycles on the PC yield and selectivity, FTIR spectra (b), UV-vis spectra (c) and TGA curves (d) of CuPc-UQA$_2$-PMO before and rafter 5 catalytic cycles.

Long-term stability and reusability are critical for practical implementation of heterogeneous catalysts. As shown in Figure 5a, CuPc-UQA$_2$-PMO retains its exceptional activity over five consecutive cycles, with the PC yield remaining consistently around 99% and no discernible loss in selectivity. This outstanding recyclability surpasses many previously reported hybrid systems prone to metal leaching or structural degradation. To probe the structural integrity after repeated use, comprehensive characterization was performed on the recovered catalyst. FTIR spectra before and after cycling (Figure 5b) show nearly identical features, with all characteristic vibrations, including those of the mesoporous skeleton, phthalocyanine ring, and quaternary ammonium groups, preserved, indicating no significant chemical decomposition or leaching. UV-vis spectrum of recycled sample (Figure 5c) still exhibits clear Q-band absorptions at 618 nm and 680 nm, confirming the retention of the intact Cu-N$_4$ coordination structure despite minor surface adsorption. TGA curves (Figure 5d) reveal matching thermal degradation profiles, further verifying the preservation of organic-inorganic architecture and thermal stability throughout the recycling process. Additionally, atomic absorption spectroscopy of the catalyst filtrates showed Cu levels below the detection limit, suggesting high stability of CuPc-UQA$_2$-PMO.

Moreover, substrate scope evaluation shows the broad applicability of CuPc-UQA$_2$-PMO across diverse epoxides (Figure S19). For small terminal epoxides such as PO and 1,2-epoxybutane, yields reach 98% and 87%, respectively, with no detectable side products. Epichlorohydrin and epibromohydrin, with reactive halogen substituents, are converted into their corresponding carbonates in 96% and 94% yields, respectively, without dehalogenation, highlighting excellent functional group tolerance. While CuPc-UQA2-PMO demonstrates broad applicability across various terminal epoxides, including those with reactive halogen substituents, it should be noted that internal epoxides with steric congestion or electronic stabilization present greater challenges. For instance, styrene oxide, the sole internal epoxide tested, afforded 80% yield after 12 hours, reflecting the combined effects of steric hindrance and resonance stabilization that impede efficient ring-opening. Although the catalyst retains activity under these conditions due to its strong cooperative activation mechanism, further increases in substrate steric bulk or substitution complexity may lead to reduced efficiency. Specially, the catalytic performance toward internal or disubstituted epoxides (e.g., cyclohexene oxide) has not been evaluated in this work. Such substrates typically exhibit lower reactivity due to increased steric hindrance around the epoxide ring, which may limit access to the active sites. Future studies will focus on optimizing the catalyst design and reaction conditions to address these more challenging substrates, potentially leveraging the synergistic activation mechanism enabled by the trinity active sites. This highlights a current limitation of the system and an important direction for future structural optimization. Nevertheless, this wide substrate compatibility underscores the versatility of the catalyst in synthesizing structurally diverse cyclic carbonates. In summary, the MPc-UQA$_x$-PMO system, particularly CuPc-UQA$_2$-PMO, functions as an efficient, stable, and reusable catalyst for solvent-free cycloaddition of CO_2 and epoxides. Its exceptional performance originates from the synergistic integration of multiple active sites, Lewis acidic Cu^{2+} centers, hydrogen-bond-donating urea groups, and iodide-releasing quaternary ammonium moieties. The CuPc unit was functionalized with triethoxysilyl groups (CuPcUTES) and subsequently incorporated into the mesoporous framework via a co-condensation strategy, designed to achieve covalent immobilization within the silica matrix. The preservation of the Q-band in UV-vis spectroscopy and characteristic FT-IR signals confirm the presence of intact CuPc moieties, while the high surface area and uniform elemental distribution suggest successful integration without aggregation. This design enables cocatalyst-free operation under mild conditions while maintaining high activity, selectivity, and recyclability,

Just Accepted

positioning it as a promising platform for sustainable CO_2 utilization in green chemical synthesis.

3.4 Catalytic reaction mechanism for MPc-UQA$_x$-PMO

To elucidate the origin of the high activity, a mechanistic study was undertaken for CuPc-UQA$_2$-PMO, combining experimental data with DFT calculations [42-44]. Based on the above experimental observations, particularly the low activity of control catalysts lacking one or more functional components, the synergistic boost from exogenous I^-, and the high performance of the fully integrated CuPc-UQA$_2$-PMO, a plausible cooperative catalytic cycle is proposed (Figure 6) [45-48]. The catalytic process initiates with the potential release of I^- species from the quaternary ammonium groups anchored within the framework, providing readily available nucleophiles essential for ring-opening (I). Concurrently, the CuPc center acts as a Lewis acid site, coordinating to the oxygen atom of PO, thereby polarizing and activating the epoxide ring. Additionally, the urea moieties incorporated into the matrix form strong hydrogen bonds with the oxygen of PO through hydrogen-bonds. This dual activation mode, Lewis acid coordination and hydrogen bonding, synergistically weakens the C-O bond strength of the epoxide, facilitating its subsequent nucleophilic attack (II). Under this cooperative activation, the released I^- preferentially attacks the less sterically hindered β-carbon of PO, triggering the nucleophilic ring-opening step and generating a stable alkoxide intermediate. This key intermediate is further stabilized by both the Cu^{2+} center and the adjacent urea group, effectively lowering the activation energy barrier of this critical transformation (III).

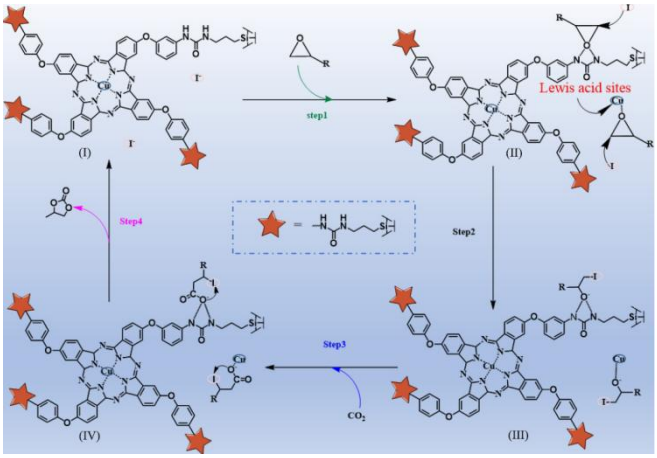


Figure 6. Proposed catalytic mechanism for CuPc-UQA$_2$-PMO.

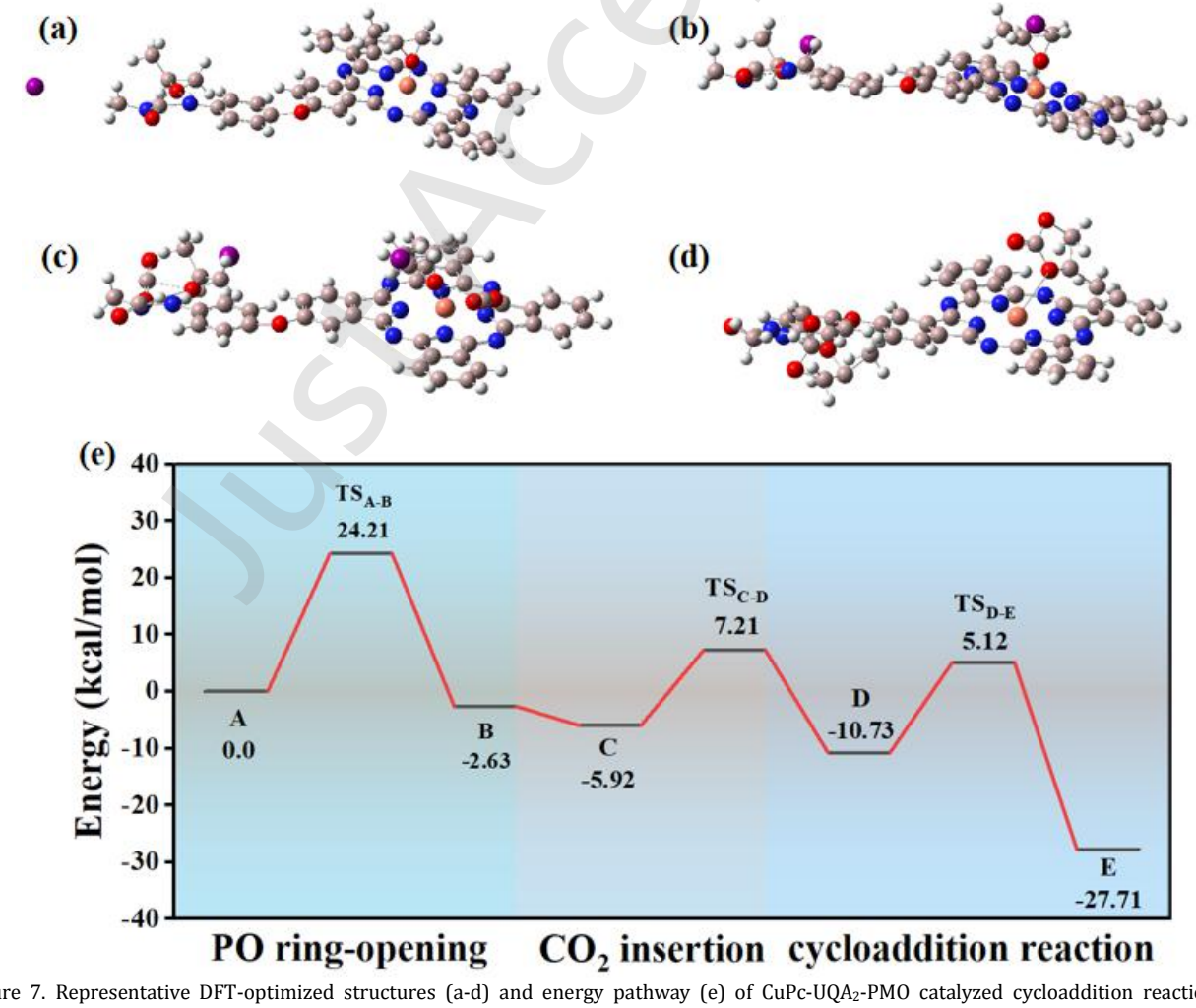


Figure 7. Representative DFT-optimized structures (a-d) and energy pathway (e) of CuPc-UQA$_2$-PMO catalyzed cycloaddition reaction. Atom colors: brown (C), red (O), blue (N), purple (I), orange (Cu), grey (H). Note: The model shown is a simplified cluster representing key functional units and does not include the full periodic mesoporous framework.

Just Accepted

Meanwhile, CO_2 molecules are activated through multiple interactions: (i) adsorption and polarization via the extended π-conjugated system of the phthalocyanine ring, which enhances the electrophilicity of the carbon atom; and (ii) electrostatic stabilization of the bent CO_2 configuration by the nearby quaternary ammonium cations, promoting its insertion into the reaction pathway. The activated CO_2 then undergoes nucleophilic addition with the alkoxide species, forming a linear alkyl carbonate intermediate (IV). Subsequently, an intramolecular cyclization occurs, accompanied by the elimination of I^-, ultimately yielding the cyclic carbonate product. After product desorption, the catalyst regenerates to its initial state, completing the catalytic cycle.

To support this proposed synergistic mechanism, DFT calculations were performed using an idealized model comprising a CuPc unit, an urea structure, as well as a free I^- ion (Figure S20) [49,50]. As shown in Figure 7, the ring-opening of the epoxide was identified as the rate-determining step (RDS), with a calculated activation energy of 24.21 kcal · mol^{-1}, which falls within a reasonable range and rationalizes the high catalytic efficiency observed under mild reaction conditions. Further analysis of the optimized transition state structures reveals the nature of the cooperative effects: (i) TSA-B (corresponding to the nucleophilic attack of I^- on the β-carbon of PO) is significantly stabilized by coordination with Cu^{2+} and hydrogen bonding from the urea group (Figure 7a, 7b); (ii) The subsequent steps, CO_2 insertion (TSC-D, Figure 7c) and intramolecular cyclization with I^- release (TSD-E, Figure 7d), exhibit relatively lower energy barriers, enabling smooth progression toward product formation; (iii) The overall energy profile (Figure 7e) clearly depicts the energetic landscape of the entire catalytic cycle, suggesting that the multi-functional cooperation substantially reduces the activation barrier compared to single-site systems. Therefore, the high catalytic activity of MPc-UQA_x-PMO originates from the synergy among multiple active sites: the Cu^{2+} center and urea group cooperatively activate the epoxide; the immobilized quaternary ammonium groups contribute I^- species that act as efficient nucleophiles to initiate ring-opening; the π-conjugated phthalocyanine scaffold and quaternary ammonium cations jointly promote CO_2 adsorption and polarization. It should be noted that the DFT model employed here is a simplified cluster approximation and does not fully account for the extended periodic structure, long-range electrostatic interactions, or confinement effects of the real mesoporous framework. Nevertheless, the calculations provide valuable atomic-level insight into the feasibility of the proposed cooperative mechanism. The computed activation energy of 24.21 kcal · mol^{-1} for the rate-determining step is consistent with the experimentally observed high activity under mild conditions, lending support to the proposed role of synergistic activation. Thus, while the model has limitations, it offers a plausible mechanistic rationale that aligns well with our experimental data. These mechanistic insights provide a solid theoretical foundation and a valuable design paradigm for developing advanced, multifunctional heterogeneous catalysts for sustainable CO_2 utilization.

4 Conclusions

In summary, we report a rational design and preparation of a multifunctional CuPc-UQA_2-PMO catalyst featuring integrated CuPc, urea, and quaternary ammonium groups. This material features the covalent integration of CuPc, urea groups, and iodide-releasing quaternary ammonium moieties within a highly ordered mesoporous silica framework, achieving a well-defined trinity catalytic architecture. Benefiting from the synergistic effect among multiple active centers, the catalyst exhibits exceptional performance for CO_2 cycloaddition with PO under co-catalyst-free conditions (100 °C, 2.0 MPa), delivering 99% yield and nearly 100% selectivity to PC. DFT calculations identify the ring-opening of PO as the rate-determining step with a calculated activation energy of 24.21 kcal · mol^{-1}. Additionally, CuPc-UQA_2-PMO demonstrates excellent recyclability, maintaining nearly unchanged catalytic activity and selectivity over five consecutive cycles, with comprehensive post-reaction characterizations indicating the structural integrity and robust anchoring of active sites. Substrate scope investigations further reveal broad applicability toward various epoxides, including halogen-substituted and sterically hindered substrates, highlighting its versatile catalytic potential. This work not only presents a highly efficient, stable, and reusable heterogeneous catalytic system for CO_2 valorization under environmentally benign conditions but also provides a rational design blueprint for integrating multiple cooperative functionalities into ordered mesoporous materials, paving the way for advanced catalysts in sustainable green chemistry and carbon resource utilization.

Electronic Supplementary Material: Supplementary material (please provide the brief detail of the ESM) is available in the online version of this article at https://doi.org/10.26599/NR.2026.94909252.

Data availability

All data needed to support the conclusions in the paper are presented in the manuscript and/or the Electronic Supplementary Material. Additional data related to this paper may be requested from the corresponding author upon request.

Acknowledgements

The financial support from Ministry of Science and Technology, China (No. 2024YFB4006704), the Open Research Fund of Key Laboratory of River Basin Digital Twinning of Ministry of Water Resources (No. KLRBDT202509) is gratefully acknowledged.

Declaration of competing interest

All the contributing authors report no conflict of interests in this work.

Author contribution statement

Just Accepted

X.F. H.: Writing-review & editing, visualization, resources, methodology. C.F. L.: Investigation, formal analysis. M.C. D.: Software, formal analysis. Y. Y.: Writing, original draft, investigation, formal analysis, data curation. Z.Y. L.: Visualization, validation. R. B. W.: Writing-review & editing, resources, funding acquisition, formal analysis, data curation. L. L. W.: Writing-review & editing, investigation, funding acquisition, formal analysis.

Informed consent

Not applicable.

Ethics statement

Not applicable.

Use of AI statement

During the preparation of this work, the authors used DeepSeek in order to polish English. After using this tool, the authors reviewed and edited the content as needed and take full responsibility for the content of the publication.

References

[1] Xiao, Z. R.;Li, P.;Zhang, H.;Zhang, S. L.;Tan, X. Y.;Ye, F.;Gu, J. M.;Zou, J. J.; Wang, D. S. A comprehensive review on photo-thermal co-catalytic reduction of CO_2 to value-added chemicals. *Fuel* **2024**, *362*, 130906.

[2] Jiang, B. W.;Liu, J.;Xiong, W. J.;Weng, M. L.;An, J. G.;Fan, Y. W.;Zheng, L. Z.;Yang, G. Q.; Zhang, Z. B. A halogen-free hyper-crosslinked ionic polymer for efficient multi-conversion of CO_2 into carbonates under mild conditions, with a combination of theoretical study. *Chem. Eng. J.* **2023**, *476*, 146873.

[3] Chen, X.;Liu, Y.;Wang, G. Q.;Kuang, Y. B.;Xiang, X. Q.;Di, G. R.;Yin, X. J.;Zhang, L.;Wang, K. X.;Cai, Q. Q. et al. Recent advances in photocatalytic CO_2 cycloaddition reaction. *Nano Res.* **2024**, *17*, 9601-9619.

[4] Wang, L. L.;Liu, Y.;Dang, Z. T.;Hou, Q. Q.;Zhang, Z. J.;Feng, Z. H.;Yu, Y.;Hua, X. F.; Wei, R. B. Rational Design of Porous Organic Polymers for Cycloaddition between Carbon Dioxide and Epoxides. *Eng. Sci.* **2025**, *35*, 1525.

[5] Fu, W. G.;Yun, Y. P.;Sheng, H. T.;Liu, X. K.;Ding, T.;Hu, S. X.;Yao, T.;Ge, B. H.;Du, Y. X.;Astruc, D. et al. Design of bifunctional single-atom catalysts NiSA/ZIF-300 for CO_2 conversion by ligand regulation strategy. *Nano Res.* **2024**, *17*, 3827-3834.

[6] Kilic, A.;Aytar, E.;Okcu, C.; Durgun, M. An improved boron-catalyzed cycloaddition of CO_2 to epoxides for the production of five-membered cyclic carbonates under atmospheric versus high-pressure conditions. *Sustainable Chem. Pharm.* **2024**, *39*, 101620.

[7] Chan, C. W.;Chen, H. L.; Chen, H. T. Synergistic Defect and Halide Catalysis for CO_2 Cycloaddition on ZIF-8: Mechanistic and Energetic Insights from Density Functional Theory. *ChemPhysChem* **2026**, *27*, e202500694.

[8] Kotanen, S.;Wirtanen, T.;Mahlberg, R.;Anghelescu-Hakala, A.;Harjunalanen, T.;Willberg-Keyrilainen, P.;Laaksonen, T.; Sarlin, E. Cyclic carbonates as building blocks for non-isocyanate polyurethanes. *J. Appl. Polym. Sci.* **2023**, *140*.

[9] Tinajero, C.;Zanatta, M.;Sánchez-Velandia, J. E.;García-Verdugo, E.; Sans, V. Reac-Discovery: an artificial intelligence–driven platform for continuous-flow catalytic reactor discovery and optimization. *Nat. Commun.* **2025**, *16*, 9062.

[10] Liu, L.;Zhang, L. L.;Chu, X.;Geng, B. K.;Wang, H. L.;Li, Z. X.;Wang, X.;Song, S. Y.; Zhang, H. J. Carbon-supported CeNCl as an efficient catalyst for CO_2 cycloaddition. *Nano Res.* **2025**, *18*, 94907028.

[11] Ren, F. Y.; Zhao, B. CO_2 Chemical Fixation into Value-Added Heterocycles Catalyzed by Non-Noble-Metal Metal-Organic Frameworks. *Acc. Chem. Res.* **2025**, *58*, 3033-3045.

[12] Ma, R.;Qiao, C. F.;Xia, L.;Xia, Z. Q.;Yang, Q.;Xu, Y. F.;Xie, G.;Chen, S. P.; Gao, S. L. Dynamic Metal-Iodide Bonds in a Tetracoordinated Cadmium-Based Metal-Organic Framework Boosting Efficient CO_2 Cycloaddition under Solvent- and Cocatalyst-Free Conditions. *Inorg. Chem.* **2022**, *61*, 7484-7496.

[13] Ma, G. H.;Chen, Y.;Li, H.;Sun, Y.;Fan, H.;Jiang, S. S.;Cui, X.; Ma, T. Y. Hierarchically porous N-doped carbon confined single-atom Fe catalyst for efficient electrochemical CO_2 reduction. *Nano Res.* **2025**, *18*, 94907297.

[14] Liu, Y. X.;Feng, Z. H.;Dang, Z. T.;Hou, Q. Q.;Yu, Y.;Zhao, X. F.;Wang, L. L.;He, Y.;Wei, R. B.; Hua, X. F. Quaternary ammonium and copper phthalocyanine functionalized polyurea heterogeneous catalysts for CO_2 and epoxides cycloaddition. *Chin. J. Chem. Eng.* **2026**, *90*, 157-167.

[15] Jin, M. M.;Niu, Q. T.;Liu, G. D.;Lv, Z. G.;Si, C. D.; Guo, H. Y. Encapsulation of ionic liquids into POMs-based metal–organic frameworks: screening of POMs-ILs@MOF catalysts for efficient cycloolefins epoxidation. *J. Mater. Sci.* **2020**, *55*, 8199-8210.

[16] Liu, L.;Zhang, J.;Cheng, X.;Xu, M.;Kang, X.;Wan, Q.;Han, B.;Wu, N.;Zheng, L.; Ma, C. Amorphous NH2-MIL-68 as an efficient electro- and photo-catalyst for CO2 conversion reactions. *Nano Res.* **2023**, *16*, 181-188.

[17] Sun, Y. X.;Zhao, T. Y.;Wang, J. J.;Yang, J. R.;Tang, H. T.;Li, W. H.; Zhang, X. Ionic liquids for CO_2 electroreduction: Structurally tunable and functionally versatile electrocatalytic platforms. *Nano Res.* **2026**, *19*, 94908332.

[18] Wang, T.;Zhu, Y. Q.;Wang, W.;Niu, J. F.;Lu, Z. Y.; He, P. L. Polyoxometalates coupled covalent organic frameworks as highly active photothermal nanoreactor for CO_2 cycloaddition. *Nano Res.* **2024**, *17*, 5975-5984.

[19] Zhao, Y. M.;Peng, Y. L.;Shan, C.;Lu, Z.;Wojtas, L.;Zhang, Z. J.;Zhang, B.;Feng, Y. Q.; Ma, S. Q. Metallocorrole-based porous organic polymers as a heterogeneous catalytic nanoplatform for efficient carbon dioxide conversion. *Nano Res.* **2022**, *15*, 1145-1152.

[20] Hu, J. W.;Qiao, W. Z.;Sun, J. J.;Xu, J.;Dong, X. Y.;Zhang, C.; Zang, S. Q. Alkynyl-anchored silver nanoclusters in lanthanide metal-organic framework for luminescent thermometer and CO_2 cycloaddition. *Nano Res.* **2023**, *16*, 7452-7458.

[21] Zhang, B. X.;Wei, T.;Chen, M. H.;Xu, Y. H.;Sun, Z. X.;Duo, M. H.; Zhang, B. Facile fabrication of pyrazine-linked metallophthalocyanine-based porous organic polymers (PyMPc-POPs) and their reduced graphene oxide (rGO) hybrids for light-driven CO_2 cycloaddition. *New J. Chem.* **2026**, *50*, 9777-9785.

[22] Hou, Q. Q.;Dang, Z. T.;Yu, Y.;Hua, X. F.;Wu, M.;Wang, L. L.; Wei, R. B. Copper phthalocyanine and ionic liquid functionalized carbon nitride for catalytic cycloaddition of carbon dioxide. *Nano Res.* **2025**, *18*,

Just Accepted

94907846.
[23] Bagherzadeh, M.;Chegeni, M.;Bayrami, A.; Amini, M. Superior and efficient performance of cost-effective MIP-202 catalyst over UiO-66-$(CO_2H)_2$ in epoxide ring opening reactions. *Sci. Rep.* **2024**, *14*, 17730.
[24] Zeng, H. C. Mesoporous Silica Encapsulated Metal-Organic Frameworks for Heterogeneous Catalysis. *Matter* **2020**, *3*, 332-334.
[25] Qin, P.;Zhang, C.;Guo, Y. Y.;Zhang, D. L.;Liu, Q.;Li, Y. D.;Song, H. B.; Lv, Z. G. Hydroxyl and amino dual-functionalized core-shell molecular sieves featuring hydrogen bond donor groups for efficient CO_2 cycloaddition. *J. Colloid Interface Sci.* **2024**, *656*, 68-79.
[26] Heydari, N.;Bikas, R.; Lis, T. Chemical CO_2 fixation by a heterogenised Zn(ii)-hydrazone complex†. *RSC Adv.* **2025**, *8*, 5977-5988.
[27] Cheng, X.;Zhao, P. H.;Zhang, M.;Wang, S. S.;Liu, M. S.; Liu, F. S. Fabrication of robust and bifunctional cyclotriphosphazene-based periodic mesoporous organosilicas for efficient CO_2 adsorption and catalytic conversion. *Chem. Eng. J.* **2021**, *418*, 129360.
[28] Lin, R. F.;Zhao, T. C.;Chen, L.;Liu, M. C.;Yu, H. Y.;Wang, R. C.;Yuan, M. J.;Li, X. M.; Zhao, D. Y. Amphipathicity mediated endocytosis of mesoporous silica nanoparticles with tunable frameworks. *Nano Res.* **2024**, *17*, 8350-8359.
[29] Liu, C. H.;Haghighat, M.;Jena, H. S.;Poelman, D.;De Geyter, N.;Morent, R.;Kaczmarek, A. M.; Van Der Voort, P. Acetylacetone functionalized periodic mesoporous organosilicas: from sensing to catalysis. *J. Mater. Chem. A* **2024**, *12*, 19137-19148.
[30] Khorasani, M.;Karimi, B.; Vali, H. Coupling of CO_2 with epoxides catalyzed by bifunctional periodic mesoporous organosilica with ionic liquid framework. *React. Chem. Eng.* **2022**, *7*, 2618-2628.
[31] Balas, M.;L, K. B.;Launay, F.; Villanneau, R. Chromium-Salophen as a Soluble or Silica-Supported Co-Catalyst for the Fixation of CO_2 Onto Styrene Oxide at Low Temperatures. *Front. Chem.* **2021**, *9*, 765108.
[32] Li, Z.;Wei, Q. Q.;Ren, Z. X.; Xie, J. Recent Progress in Heteroatom-Containing Metalloporphyrin-Based Catalysts for CO_2 Reduction. *MOLECULES* **2025**, *30*, 2287.
[33] Joudian, S.;Todisco, S.;Mastrorilli, P.; Khorasani, M. Room-Temperature and Atmospheric Pressure Coupling of Carbon Dioxide with Epoxides Catalyzed by Iodide Ions Confined in Nanopores of Periodic Mesoporous Organosilica. *ACS Appl. Nano Mater.* **2025**, *8*, 7394-7406.
[34] Wang, L. L.;Feng, Z. H.;Hou, Q. Q.;Dang, Z. T.;Yu, Y.;Yang, C.;Tang, B.;Zhou, Q. C.;Hua, X. F.;Wei, R. B. et al. Quaternary ammonium salt functionalized copper phthalocyanine-graphene oxide hybrids for cocatalyst-free carbon dioxide cycloaddition. *Adv. Compos. Hybrid Mater.* **2024**, *8*, 40.
[35] Wei, R. B.;Jiao, Y. Y.;Liu, Y. X.;Wang, Z. X.;Zhao, X. F.;Bao, S. M.;Wang, L. L.;Dang, Z. M.;Zheng, X. Y.; Hua, X. F. Hot stretching induced Orientation of Calcium Copper Titanate Nanorods in Polyetherimide for Enhanced Energy Storage Density. *Small* **2026**, *22*, e13033.
[36] Wei, R.;Liu, Y.;Gao, F.;Feng, Z.;Huo, Q.;Liu, K.;Zhang, Z.;Lei, X.; Wang, L. Enhancing high-temperature energy storage performance of poly(arylene ether nitrile) hybrids synergistically via phthalonitrile modified boron nitride and carbon nanotube. *Adv. Compos. Hybrid Mater.* **2024**, *7*, 50.
[37] Wei, R. B.;Wang, Z. X.;Jiao, Y. Y.;Liu, Y. X.;Bao, S. M.;Wang, L. L.;Hua, X. F.; Wang, X. Enhancing Dielectric Energy Storage Properties of Poly(Arylene Ether Nitrile) Via Controlling the Distribution of Boron Nitride Nanosheets. *Adv. Funct. Mater.* **2026**, *36*, e19368.
[38] Feng, Z. H.;Tang, B.;Liu, K. X.;Hou, Q. Q.;Dang, Z. T.;Yang, C.;Hua, X. F.;Yu, Q. s.;Wang, L. L.; Wei, R. B. One-pot synthesis of copper phthalocyanine polymer: An efficient CO_2 fixation catalyst. *Mater. Today Commun.* **2024**, *41*, 110875.
[39] Zhang, Y. P.;Liang, H. G.;Li, X. Y.;Li, Q. F.; Wang, J. W. Melem based mesoporous metal-free catalyst for cycloaddition of CO_2 to cyclic carbonate. *J. CO2 Util.* **2022**, *64*, 102173.
[40] Liu, M. S.;Zhao, P. H.;Zhang, W. W.;Cheng, X.;Fei, H. T.;Ma, J. J.; Liu, F. S. Rational self-assembly of triazine- and urea-functionalized periodic mesoporous organosilicas for efficient CO_2 adsorption and conversion into cyclic carbonates. *Fuel* **2022**, *315*, 123230.
[41] Hernández, E.;Navarro, P.;Pescarmona, P. P.; Palomar, J. Dissociation role on the catalytic activity of organic halides in CO_2 conversion to cyclic carbonates: Experimental and computational study. *J. CO2 Util.* **2024**, *88*, 102929.
[42] Wei, R. B.;Huo, Q.;Liu, K. X.;Elnaggar, A. Y.;El-Bahy, S. M.;El-Bahy, Z. M.;Ren, J. N.;Wang, L. L.; Wu, Z. J. Distributing fluorinated carbon nanotube on pore walls of polyarylene ether nitrile porous films for advanced electromagnetic interference shielding. *Adv. Compos. Hybrid Mater.* **2024**, *7*, 196.
[43] Wei, W. S.;Wang, Y. X.;Xu, G. W.;Zhao, J. G.; Shi, L. Construction of multifunctionally integrated catalyst via a self-assembly strategy for efficient CO_2 cycloaddition. *Fuel* **2025**, *388*, 134499.
[44] Wei, R. B.;Gao, F.;Hou, H.;Xu, B. B.;Yang, H. Y.;Zhang, X.;Guo, Z. H.; Wang, L. L. Triazine and urea constructed polyurea microsphere as a promising catalyst for CO_2 conversion to cyclic carbonates. *J. Environ. Chem. Eng.* **2025**, *13*, 116312.
[45] Shi, Z. J.;Su, Q.;Ying, T.;Tan, X.;Deng, L. L.;Dong, L.; Cheng, W. G. Ionic liquids with multiple active sites supported by SBA-15 for catalyzing conversion of CO_2 into cyclic carbonates. *J. CO2 Util.* **2020**, *39*, 101162.
[46] Guo, L. P.;Lamb, K. J.; North, M. Recent developments in organocatalysed transformations of epoxides and carbon dioxide into cyclic carbonates. *Green Chem.* **2021**, *23*, 77-118.
[47] Yan, Q. Q.;Liang, H.;Wang, S. L.;Hu, H.;Su, X. F.;Xiao, S. T.;Xu, H. J.;Jing, X. C.;Lu, F.; Gao, Y. N. Immobilization of Ionic Liquid on a Covalent Organic Framework for Effectively Catalyzing Cycloaddition of CO_2 to Epoxides. *MOLECULES* **2022**, *27*, 6204.
[48] Gonzalez, A. C. S.;Felgueiras, A. P.;Aroso, R. T.;Carrilho, R. M. B.; Pereira, M. M. Al(III) phthalocyanine catalysts for CO_2 addition to epoxides: Fine-tunable selectivity for cyclic carbonates versus polycarbonates. *J. Organomet. Chem.* **2021**, *950*, 121979.
[49] R.B. Wei, S.M. Bao, Y.X. Liu, X.F. Zhao, Y. Yu, C.F. Lai, L.L. Wang, X.F. Hua. Fabrication of multilayer alternating polymer-based dielectric composites with superior energy storage performance via layer-bylayer spraying assembly. *Nano Research Energy*, **2026**, e9120269.
[50] Cai, K. X.;Liu, P.;Chen, Z.;Chen, P.;Liu, F.;Zhao, T. X.; Tao, D. J. Construction of bifunctional triazine-based

Just Accepted

imidazolium porous ionomer polymers by a post-crosslinking tactic for efficient CO_2 capture and conversion. *Chem. Eng. J.* **2023**, *451*, 138946.

© The Author(s) 2026. *Nano Research* published by Tsinghua University Press. The articles published in this open access journal are distributed under the terms of the Creative Commons Attribution 4.0 International License (http://creativecommons.org/licenses/by/4.0/), which permits use, distribution and reproduction in any medium, provided the original work is properly cited

Just Accepted

Electronic Supplementary Material

Design of periodic mesoporous organosilica catalyst bearing copper phthalocyanine and quaternary ammonium for CO_2 cycloaddition

Xiufu Hua[1,2], Chunfang Lai[1], Mengchi Dai[1], Yue Yu[1], Zhongyuan Liang[1], Renbo Wei[1], Lingling Wang[1]

[1] *Institute of Low-Carbon Technology Application, School of Chemical Engineering, Northwest University, Xi'an 710069, China*
[2] *Yangtze Delta Region Institute of Tsinghua University, Jiaxing 314006, China*

Supporting information to https://doi.org/10.26599/NR.2026.94909252

Just Accepted

Address correspondence to X. Hua, huaxf@nwu.edu.cn; L. Wang, wangll@nwu.edu.cn

Materials

4-Aminobenzonitrile (4-APN) was synthesized according to methods reported in the literature. 4-Aminophenyl isocyanate, 4-nitrophthalonitrile, N,N-diisopropylethylamine (DIPEA), propyl triethoxysilane isocyanate, tetrabutylammonium iodide (TBAI), tetrabutylammonium chloride, tetrabutylammonium bromide, 1,2-epoxyhexane, anhydrous copper(II) chloride ($CuCl_2$), potassium sulfide, and anhydrous ethanol were all purchased from Adamas Reagents. N,N-dimethylformamide (DMF), N,N-dimethylacetamide (DMAc), and potassium carbonate (K_2CO_3) were obtained from Tianjin Damiao Chemical Reagent Factory. Cetyltrimethylammonium bromide (CTAB), bis(triethoxysilyl)ethane (BTEE), and 3-chloropropyltriethoxysilane (CPTES) and potassium bromide were obtained from Shanghai Macklin Biochemical Technology Co., Ltd. Propylene oxide (PO), 1,2-epibutane, and styrene oxide were all obtained from Shanghai Aladdin Biochemical Technology Co., Ltd. CO_2 (99.99%) was supplied by the Xi'an Chang'an District Oxygen Station in China. Further information on the raw materials can be found in the ESM.

Just Accepted

Characterization

The FTIR spectra of TDI and MPc-UQA$_x$-PMO were collected with a BRUKER VERTEX70 TGA-IR instrument, whereby the samples were placed onto KBr pellets. The microstructure of MPc-UQA$_x$-PMO was observed using a SIGMA FE scanning electron microscope (SEM). The SEM observation was performed at 5.0 KV after gold spraying, during which the SEM mapping micrographs were also obtained. Thermo Fisher Nexsa X-ray photoelectron spectroscopy (XPS) was used to determine the elemental composition of MPc-UQA$_x$-PMO, employing a monochromatic Al Kα (hν=1486.8 eV) X-ray source. Thermal gravimetric analysis of the MPc-UQA$_x$-PMO was carried out using a TA Instrument TGA-Q50 with a heating rate of 20 ^{o}C/min from room temperature to 800 ^{o}C under a nitrogen atmosphere. The N_2 adsorption-desorption isotherms of the degassed MPc-UQA$_x$-PMO (120 ^{o}C, 6 h) was tested at 77 K with the Micromeritics ASAP 2420 adsorption analyzer. The surface area and pore-size distributions of MPc-UQA$_x$-PMO were calculated basing on the N_2 adsorption-desorption isotherms by using the Brunauer-Emmett-Teller (BET) equation and Barrett-Joyner-Halenda (BJH) model.

Just Accepted

Gas chromatography (GC) analysis was performed on a GC-7900 (Shanghai Tianmei) equipped with a capillary column (OV-17, 30 m×0.53 mm×1.0 μm) and a FID detector. The analytical conditions are as follows: injector temperature at 220 °C; detection temperature at 260 °C; sample volume 0.2 μL; column temperature is programmed (at 60 °C for 1 min in the beginning, heating to 220 °C at the rate of 10 °C/ min, and then keeping at 220 °C for 1 min). The yield, conversion, selectivity are calculated by the following Equations:

$$\text{Yield} = A1 / (A1 + A2 + A3) \times 100\% \quad (1)$$

$$\text{Conversion} = (A_1+A_2) / (A_1+A_2+A_3) \times 100\% \quad (2)$$

$$\text{Selectivity} = A_1 / (A_1+A_2) \times 100\% \quad (3)$$

where A_1 is peak area of the target product, A_2 represents the total peak areas of the by-products, A_3 means the peak area of the residue epoxide, basing on the GC curve.

Just Accepted

Synthesis of 4-aminophenoxyphthalonitrile (4-APN)

Nitropathalonitrile (8.6 g, 0.05 mol), 4-aminophenol (5.5 g, 0.05 mol), anhydrous potassium carbonate (8.5 g, 0.06 mol), and DMSO (100 mL) were mixed using a stirrer. After refluxing at 80 °C for 10 h, the reaction mixture was cooled to RT and then poured into distilled water. The products were filtered and washed several times with distilled water. The product was dried at 60 °C for 12 h after recrystallization from acetone/water mixed solvents (yield: 90 %).

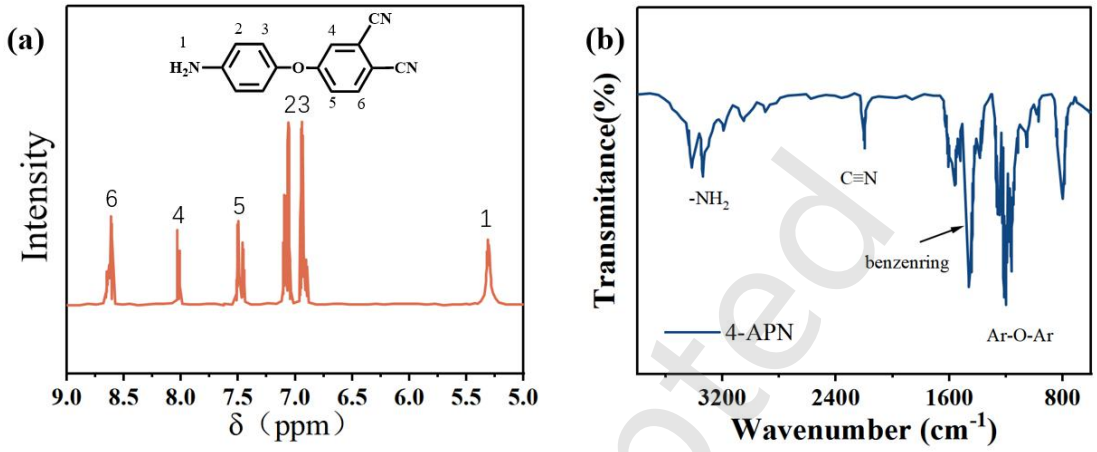


Figure S1. ^{1}H NMR spectrum (a) and FTIR (b) of 4-APN.

Just Accepted

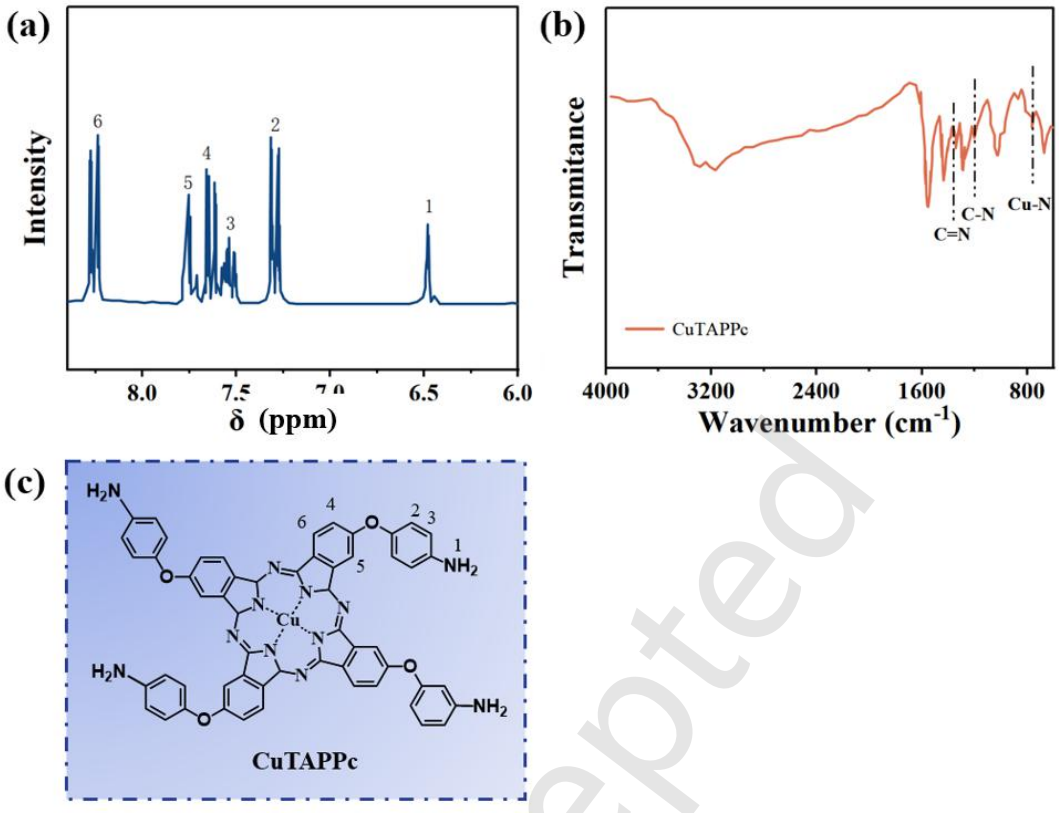


Figure S2. ^{1}H NMR spectrum (a), FTIR (b) and structure (c) of CuTAPPc.

Just Accepted

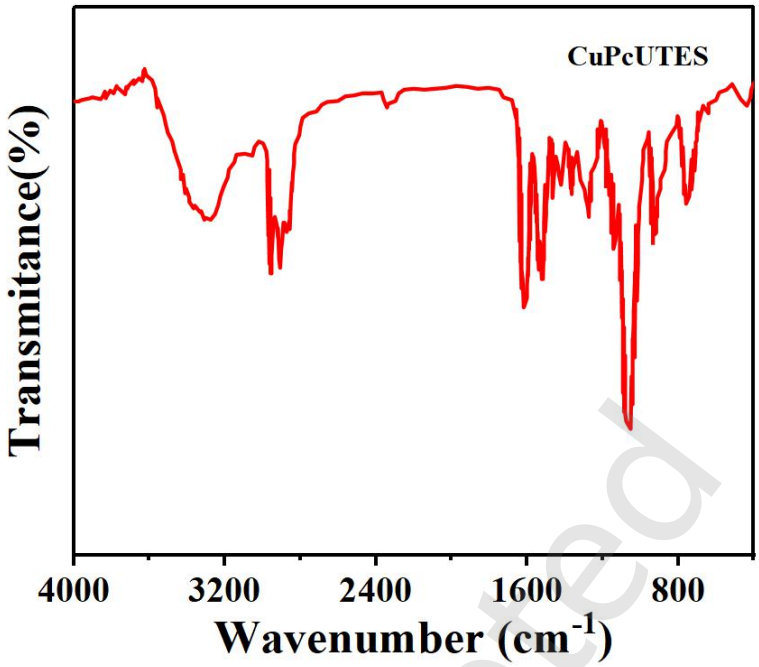


Figure S3. FTIR spectrumof CuPcUTES.

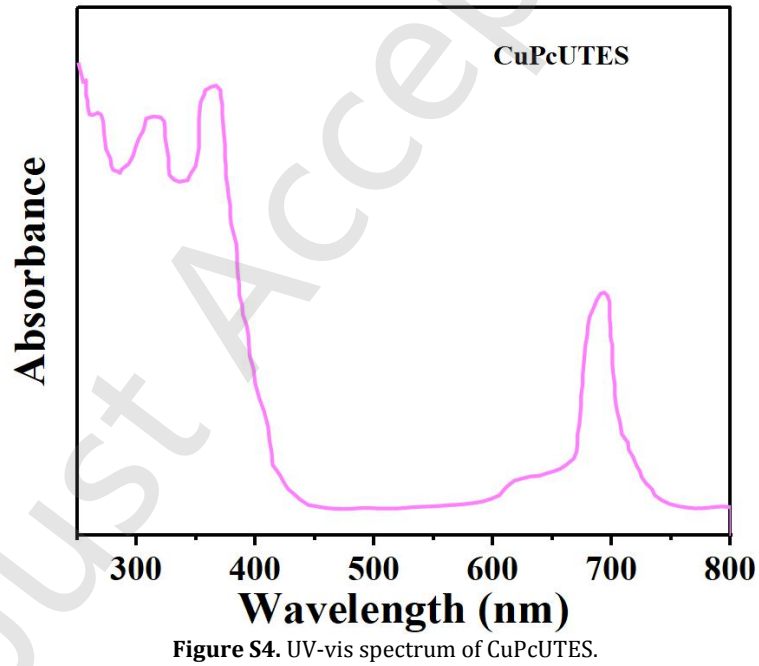


Figure S4. UV-vis spectrum of CuPcUTES.

Just Accepted

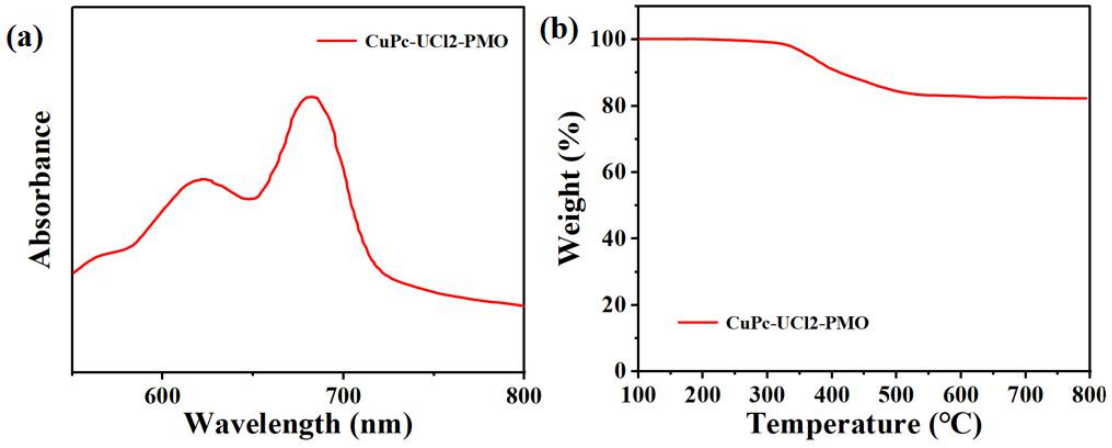


Figure S5. UV-vis spectrum (a) and TGA curve (b) of CuPc-UCl_2-PMO.

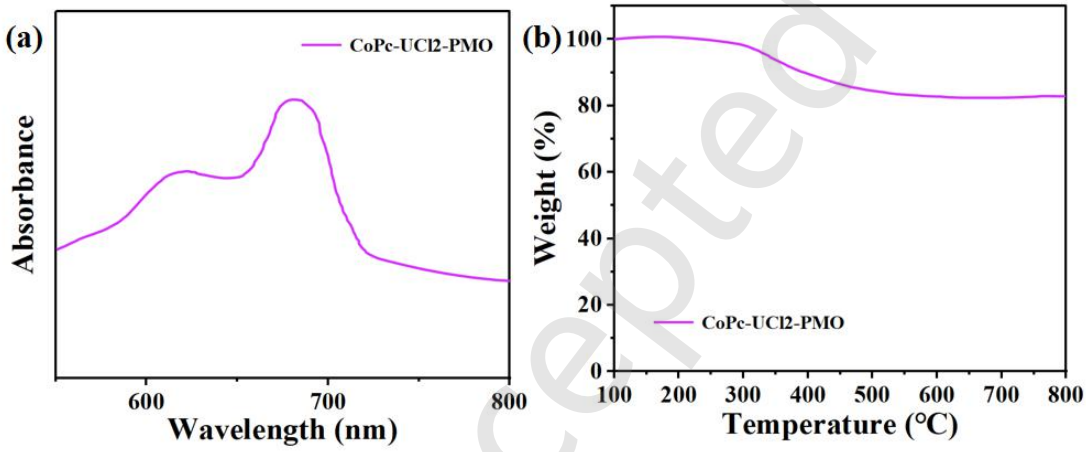


Figure S6. UV-vis spectrum (a) and TGA curve (b) of CoPc-UCl_2-PMO.

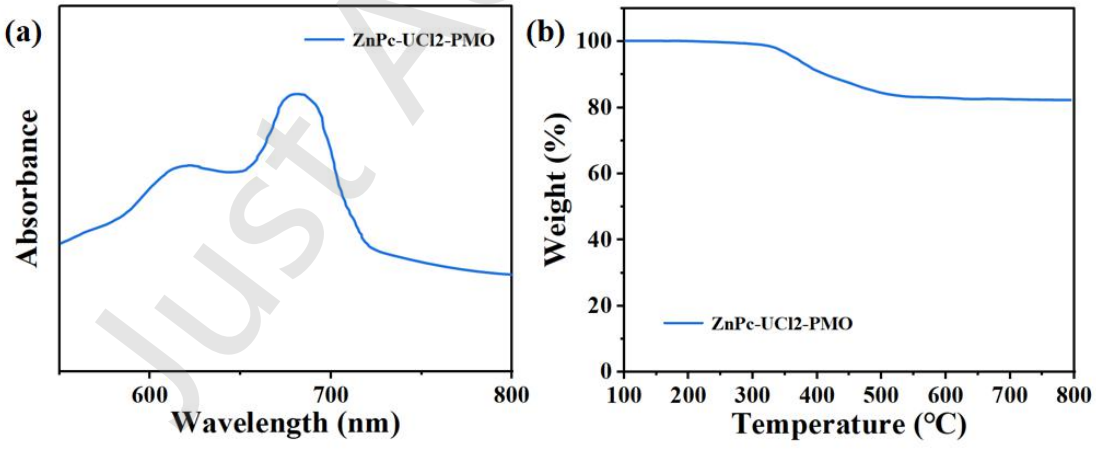


Figure S7. UV-vis spectrum (a) and TGA curve (b) of ZnPc-UCl_2-PMO.

Just Accepted

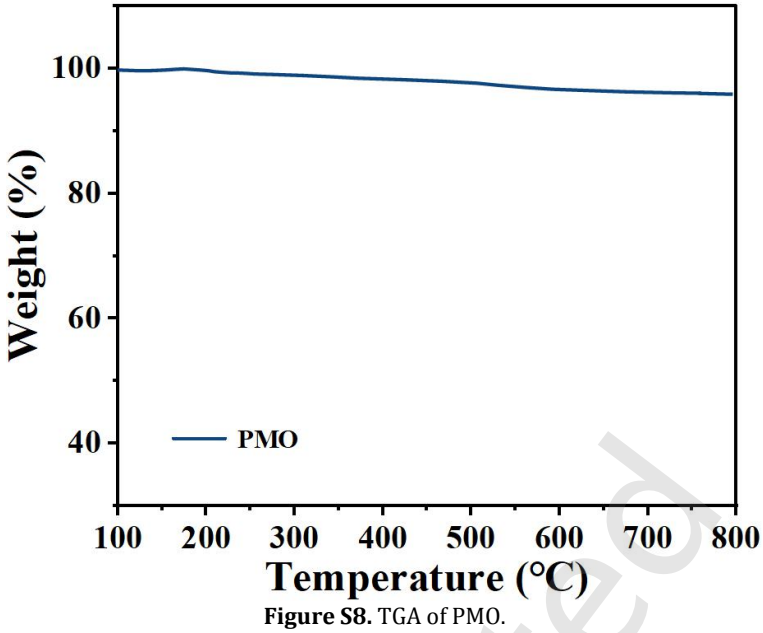


Figure S8. TGA of PMO.

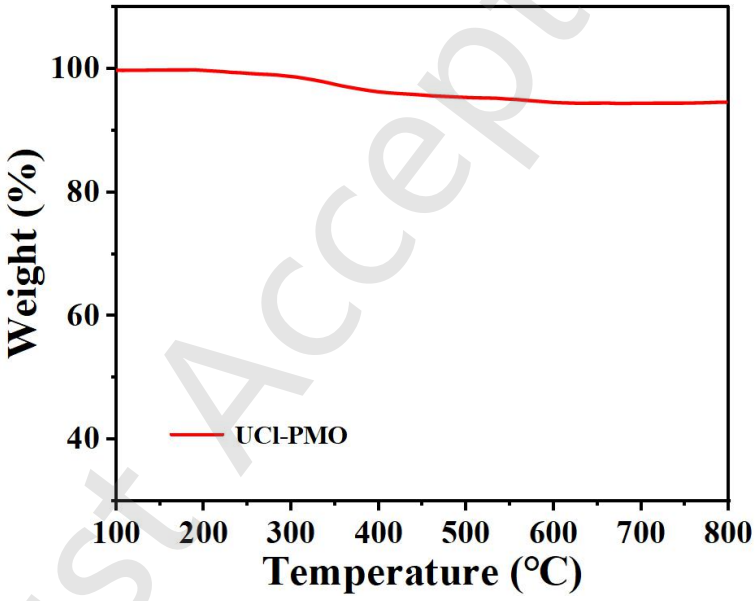


Figure S9. TGA of UCl-PMO.

Just Accepted

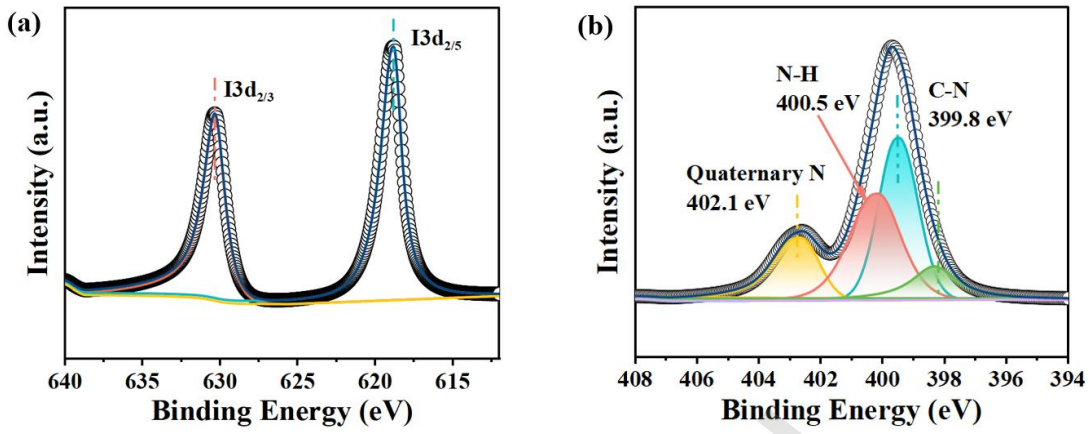


Figure S10. (a) I 3d and (b) N 1s XPS spectra of CuPc-UQA-PMO.

Just Accepted

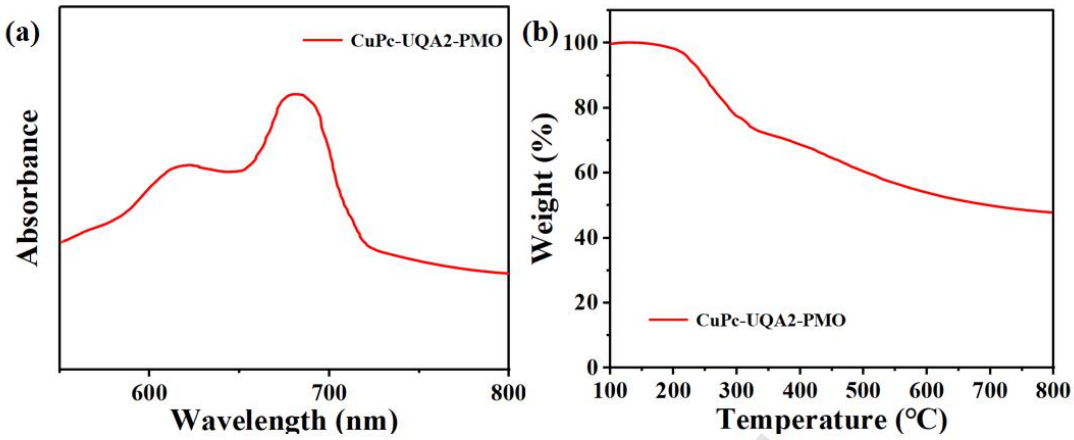


Figure S11. UV-vis spectrum (a) and TGA curve (b) of CuPc-UQA$_2$-PMO.

Just Accepted

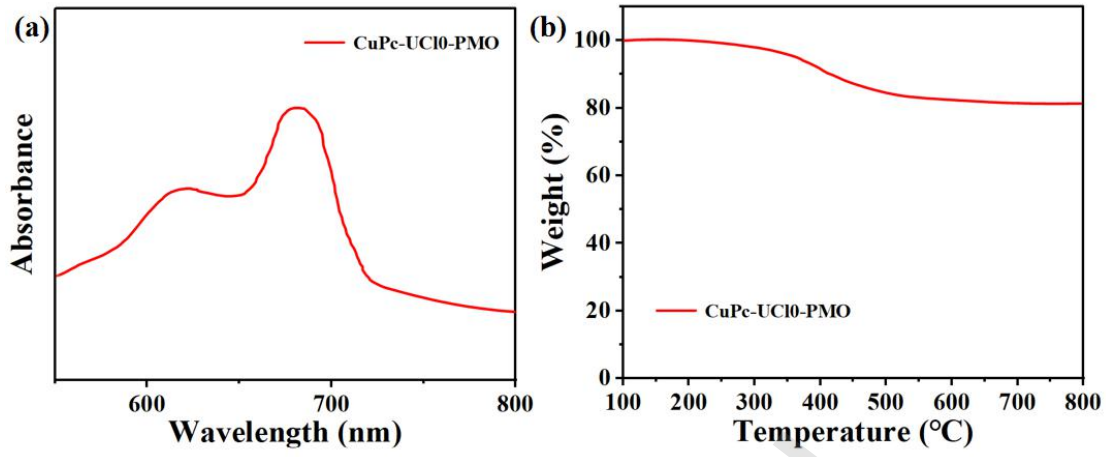


Figure S12. UV-vis spectrum (a) and TGA curve (b) of CuPc-UCl_0-PMO.

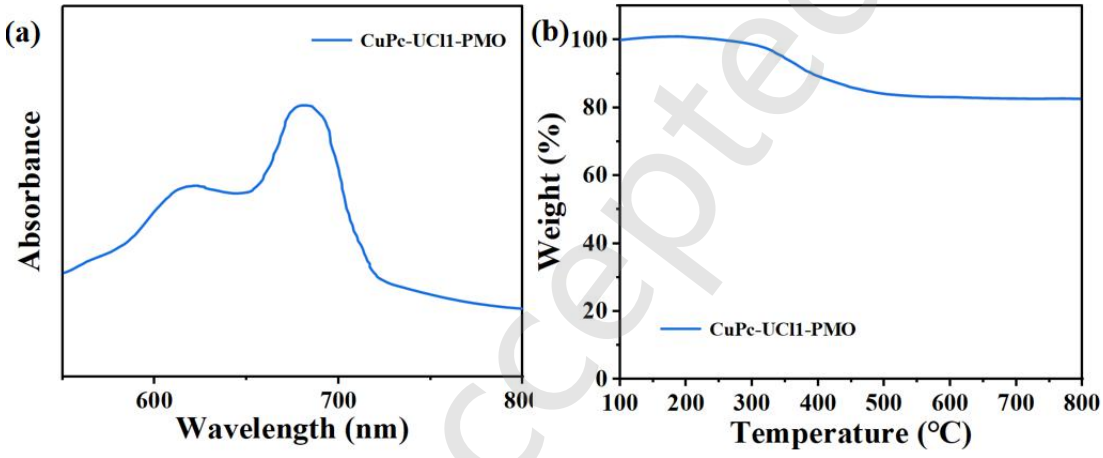


Figure S13. UV-vis spectrum (a) and TGA curve (b) of CuPc-UCl_1-PMO.

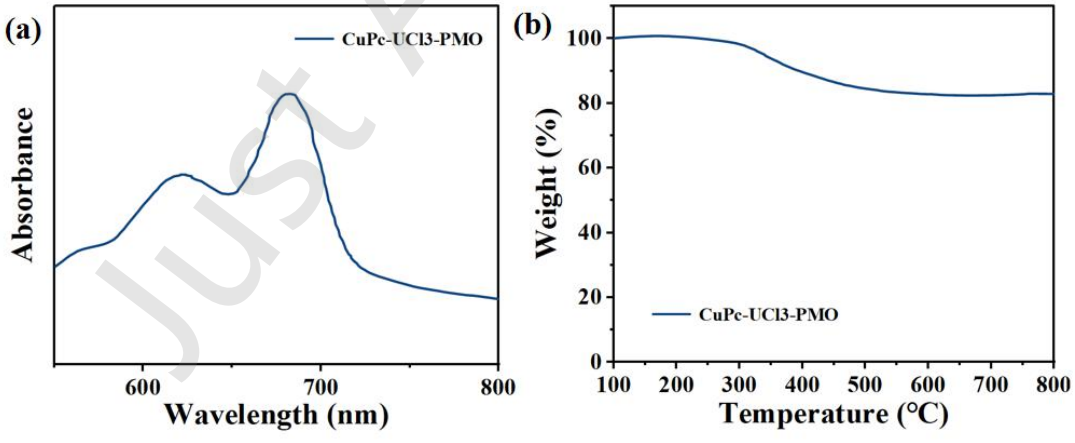


Figure S14. UV-vis spectrum (a) and TGA curve (b) of CuPc-UCl_3-PMO.

Just Accepted

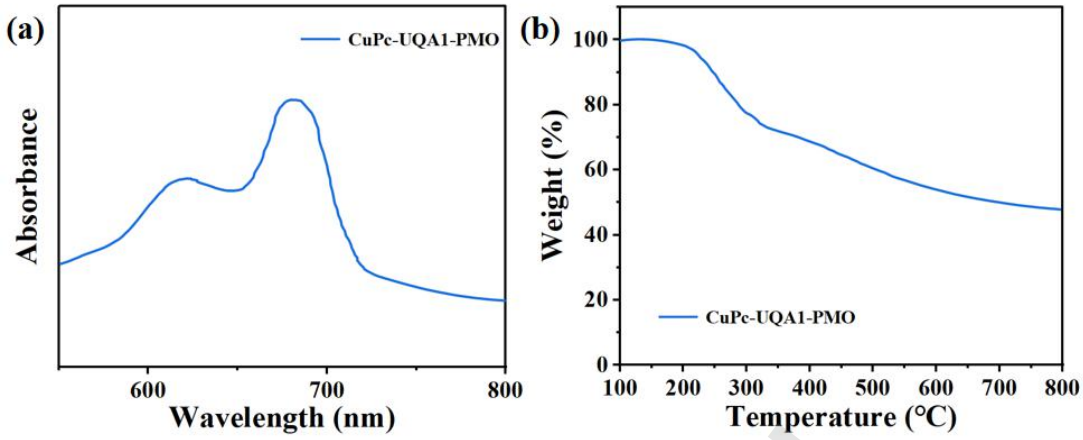


Figure S15. UV-vis spectrum (a) and TGA curve (b) of CuPc-UQA$_1$-PMO.

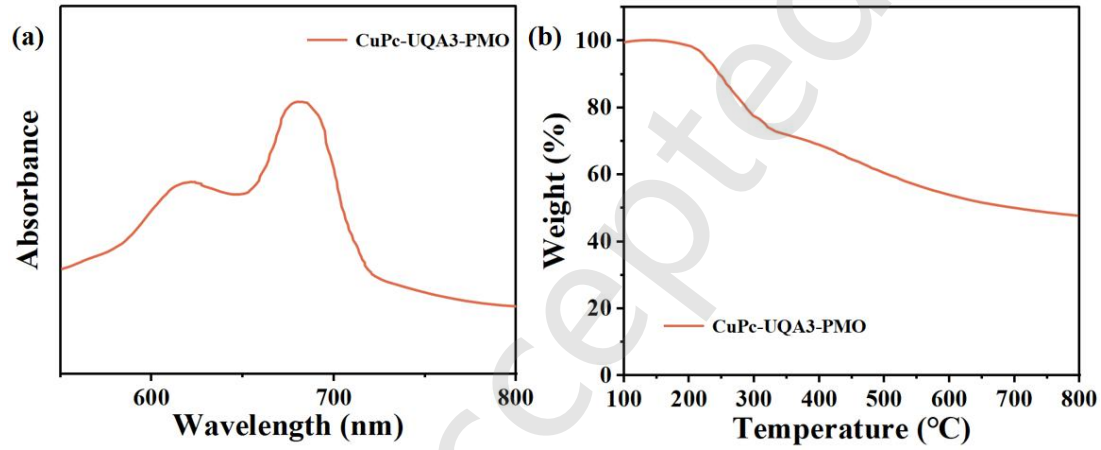


Figure S16. UV-vis spectrum (a) and TGA curve (b) of CuPc-UQA$_3$-PMO.

Just Accepted

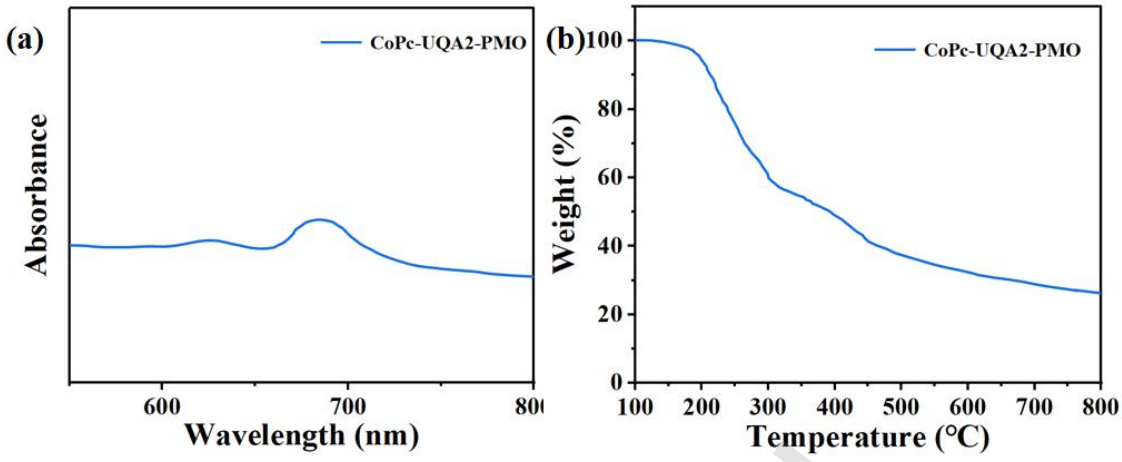


Figure S17. UV-vis spectrum (a) and TGA curve (b) of CoPc-UQA$_2$-PMO.

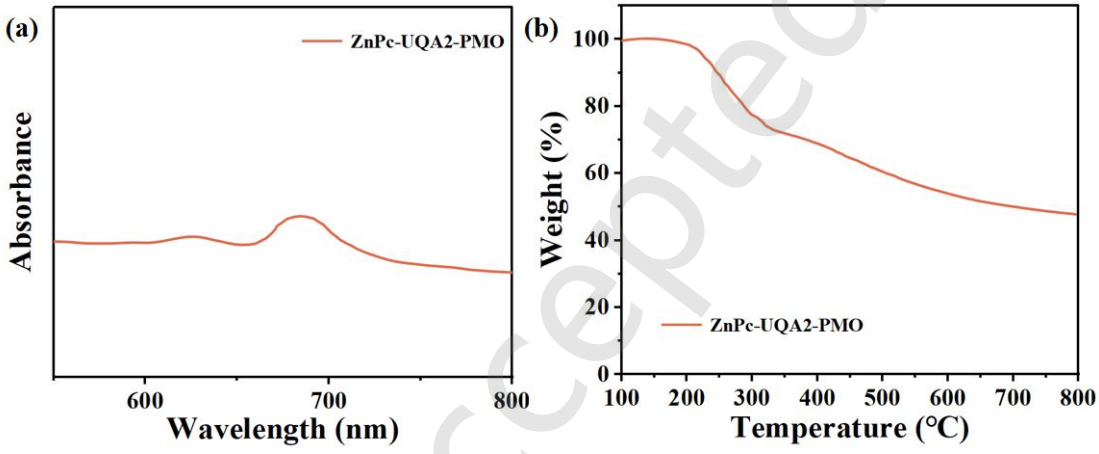


Figure S18. UV-vis spectrum (a) and TGA curve (b) of ZnPc-UQA$_2$-PMO.

Just Accepted

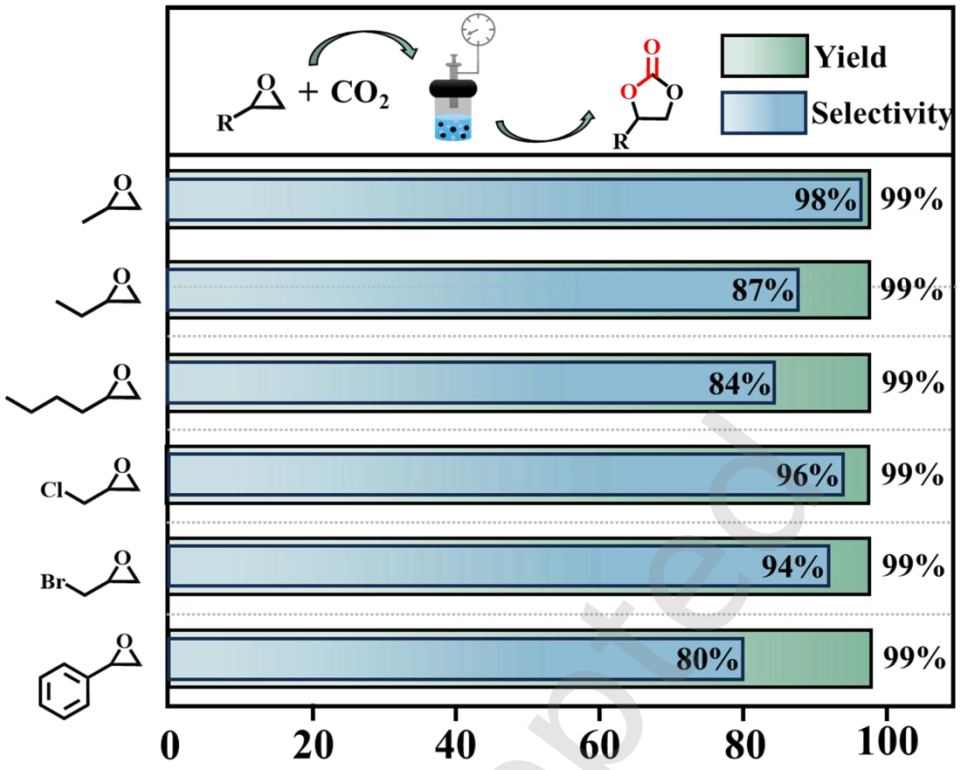


Figure S19. Versatility of the CuPc-UQA$_2$-PMO. The reaction conditions are as follows: the amount of epoxide 30 mmol, CuPc-UQA$_2$-PMO, 7 wt%, CO_2, pressure 2.0 MPa, 90 ℃, 10 h.

Just Accepted

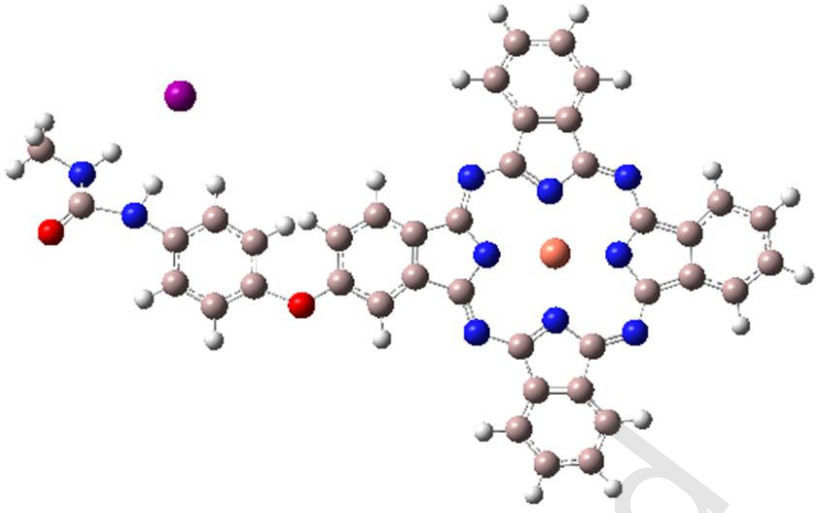


Figure S20. Simplified model of CuPc-UQA-PMO for DFT calculation.

Just Accepted

Table S1. Comparison of representative heterogeneous catalysts for CO_2/epoxide cycloaddition.

Entry	Catalyst	Epoxide	Catalyst loading	Cocatalyst	Temperature (°C)	CO2 pressure (MPa)	Time (h)	Yield (%)	Selectivity (%)	TOF (h^{-1})	Ref.
1	I@BFPMO-IL	PO	1 mol%	None	70	1	3	98	N.R.	33	S1
2	I-BIm-PMO	PO	4 mol%	None	RT	0.1	18	99	N.R.	N.R.	S2
3	PMO-CPF-20	PO	5.0 wt% (vs PO)	TBAI, 0.78 mol% (vs PO)	90	2	6	98	>=99	N.R.	S3
4	TUF-PMO-20	PO	5.0 wt% (vs PO)	TBAI, 0.78 mol% (vs PO)	90	1.5	4	99	99	N.R.	S4
5	GO-CuPc-IL	PO	3.0 wt% (vs PO)	None	100	1.5	8	98	99	N.R.	S5
6	PU-CuPc-QA	PO	6.0 wt% (vs PO)	None	100	1.5	6	99	99	N.R.	S6
7	C3N4-CuPc-IL	PO	5.0 wt% (vs PO)	None	120	2	12	98	99	N.R.	S7
8	MIL-101-ILs(COOH)	PO	150 mg (0.26 mol%)	None	80	1	6	86	N.R.	N.R.	S8
9	COF-50%QA	ECH	0.5 mol%	None	100	0.1	16	98	>99	8.2	S9
10	CuPc-UQA_2-PMO	PO	7.0 wt% (vs PO)	None	100	2	10	99	99	118	This work

Notes: N.R. = not reported. Catalyst loading is reported as given in the original literature (e.g., wt%, mol%, or mg). TON/TOF values are listed only when explicitly reported by the original authors.

References

[S1] M. Khorasani, B. Karimi, H. Vali. Coupling of CO_2 with epoxides catalyzed by bifunctional periodic mesoporous organosilica with ionic liquid framework. *React. Chem. Eng.* **2022**, *7*, 2618-2628.

[S2] S. Joudian, S. Todisco, P. Mastrorilli, M. Khorasani. Room-Temperature and Atmospheric Pressure Coupling of Carbon Dioxide with Epoxides Catalyzed by Iodide Ions Confined in Nanopores of Periodic Mesoporous Organosilica. *ACS Appl. Nano Mater.* **2025**, *8*, 7394-7406.

[S3] X. Cheng, P.H. Zhao, M. Zhang, S.S. Wang, M.S. Liu, F.S. Liu. Fabrication of robust and bifunctional cyclotriphosphazene-based periodic mesoporous organosilicas for efficient CO_2 adsorption and catalytic conversion. *Chem. Eng. J.* **2021**, *418*, 129360.

[S4] M.S. Liu, P.H. Zhao, W.W. Zhang, X. Cheng, H.T. Fei, J.J. Ma, F.S. Liu. Rational self-assembly of triazine- and urea-functionalized periodic mesoporous organosilicas for efficient CO_2 adsorption and conversion into cyclic carbonates. *Fuel* **2022**, *315*, 123230.

[S5] L.L. Wang, Z.H. Feng, Q.Q. Hou, Z.T. Dang, Y. Yu, C. Yang, B. Tang, Q.C. Zhou, X.F. Hua, R.B. Wei, T.X. Liu. Quaternary ammonium salt functionalized copper phthalocyanine-graphene oxide hybrids for cocatalyst-free carbon dioxide cycloaddition. *Adv. Compos. Hybrid Mater.* **2025**, *8*, 15.

[S6] Y.X. Liu, Z.H. Feng, Z.T. Dang, Q.Q. Hou, Y. Yu, X.F. Zhao, L.L. Wang, Y. He, R.B. Wei, X.F. Hua Quaternary ammonium and copper phthalocyanine functionalized polyurea heterogeneous catalysts for CO_2 and epoxides cycloaddition. *Chin. J. Chem. Eng.* **2026**, *90*, 157-167.

[S7] Q.Q. Hou, Z.T. Dang, Y. Yu, X.F. Hua, M. Wu, L.L. Wang, R.B. Wei. Copper phthalocyanine and ionic liquid functionalized carbon nitride for catalytic cycloaddition of carbon dioxide. *Nano Res.* **2025**, *18*, 94907846.

[S8] Y. Chen, F.F. Li, L.Y. Liu, Y.H. Zhou. Implanting multi-functional ionic liquids into MOF nodes for boosting CO_2 cycloaddition under solventless and cocatalyst-free conditions. *Chem. Eng. J.* **2024**, *490*, 151657.

[S9] J. Huang, S. Peng, Y. Du, J. Feng, J. Li, J. Su, G. Zhang. Quaternary Ammonium-Functionalized Mesoporous Covalent Organic Frameworks for Effective Catalytic CO_2 Cycloaddition. *ACS Applied Polym. Mater.* **2024**, *6*, 4607-4614.

Just Accepted